Mapping post-translational histone modifications and the TH2B variant in spermatogenesis

By

Camilla Holmsen

Master in molecular medicine

Department of Cancer Research and Molecular Medicine

NTNU

Master thesis, carried out at the Centre for Molecular Biology and Neurosciene, Institute of Medical Microbiology, Oslo University Hospital, Rikshospitalet

July, 2012

CENTRE FOR MOLECULAR BIOLOGY AND NEUROSCIENCE
Senter for molekylærbiologi og nevrovitenskap

Oslo University Hospital

AKNOWLEDGEMENT

The work presented in this thesis was carried out from August 2011 – July 2012 at the Institute for Medical Molecular Biology and Centre for Molecular Biology and Neuroscience (CMBN) at Oslo university Hospital Rikshospitalet. The thesis is a part of the master program in Molecular Medicine at the Norwegian University of Science and Technology.

First of all, I would like to thank my supervisor post doc John-Arne Dahl for his proficient supervision and for always being so positive on my behalf. He offered me professional advice, support and suggestion and taught me the versatile ChIP assay and always helped me when I was uncertain. Furthermore, I want to thank him for support in my writing and critical proofreading of my thesis. Thank you so much for your excellent guidance!

Furthermore, I would like to thank Prof. Arne Klungland for offering me the possibility to perform my Master Thesis in his laboratory.

My appreciation also goes to Kari Furu for teaching me the STA-PUT technique, the immunofluorescence staining procedure and the Axio Observer.Z1 microscope. Moreover, I want to thank all members of Arne Klungland`s group and Magnar Bjørås group for always being helpful and friendly.

Special thanks go to Kristine Kjeldal and Sheba Lothe my colleagues and friends at the laboratory of Molecular Cancer Genetics. Thank you Kristine for inspire me to take this master, for many vital morning coffee at the "Kaffebrenneriet" and for always listening to me when I was frustrated. Sheba you always support me and give me good advices.

I want to thank my friends for all support throughout this year, and last but not least I want to thank my brother Martin, my father Petter and my mother Grete for always being caring and supportive and always believe in me.

Oslo, july 2012

Camilla Holmsen

ABSTRACT

Epigenetics has been defined by Goldberg et al. [1] as the study of heritable changes in gene expression or cellular phenotype which arises without changes in the DNA sequence. Post-translational histone modification and exchange of histone variants are two important epigenetic mechanisms. Histones and histone variants have been shown to be involved in many cellular events, for example they largely contribute to regulation of gene expression.

Chromatin immunoprecipitation (ChIP) is a versatile tool to study protein-DNA interactions in general and the location of post-translational histone modifications in particular. We used this approach to investigate three post-translational histone modifications and a histone variant, during spermatogenesis where global changes in the epigenome are known to occur.

We assessed occupancy of the histone modifications H3K4me3, H3K9me2 and H3K27me3 and the testis specific histone variant TH2B on regulatory sequences of genes encoding histone modifying enzymes, chromatin remodelers and genes important to early embryo development in mice pachytene spermatocytes (PCS) and round spermatids (RS).

The objective of this thesis was to initiate the investigation of the role of TH2B and the bivalent marks H3K27me3 and H3K4me3 in spermatogenesis. This study revealed that the facultative repressive mark H3K9me2 and TH2B showed strong correlation at gene regulatory sequences in PCS and RS cells. Moreover, TH2B correlated inversely with the activating mark H3K4me3. This may indicate that TH2B plays a role as a testis specific repressive histone variant. Additionally, we observed significant levels of the bivalent marks H3K4me3 and H3K27me3 on the *Hoxd4* and *Oct4* promoter in PCS and RS. On a speculative note, this could perhaps be suggestive of preprogramming for expression in early embryo development.

ABBREVIATIONS

A260	absorbance of UV-light at 260 nm
ADP	Adenosine diphosphate
ATP	adenosine triphosphate
ATR	ataxia telangiectasia and Rad3 related protein
ATTC	American Type Culture Collection
BGI	Bejing Genomics Institute
bp	base pairs
BRCA1	breast cancer type 1 susceptibility protein
BSA	Bovine serum albumine
cDNA	complementary DNA
ChIP	chromatin immunoprecipitation
ChIP-seq	ChIP sequencing
CpG	cytosine-phosphate-guanine
DAPI	4',6-diamidino-2-phenylindole, dihydrochloride
DEPC water	diethylpyrocarbonate treated water
DMEM	Dulbecco's Modified Eagle Medium
DNA	Deoxyribonucleic acid
DNMT	DNA methyltransferase
DSB	double-strand break
dsDNA	double stranded DNA
E	glutamate
EDTA	etylendiaminetetraacetic acid
ES cell	embryonic stem cell
FAD	flavin adenine dinucleotide
H1	histone 1
H2A	histone 2A
H2B	histone 2B
H3	histone 3
H3K27me3	Tri-Methylated Histone H3 at Lysine 27
H3K4me3	Tri-Methylated Histone H3 at Lysine 4
H3K9me2	Di-Methylated Histone H3 at Lysine 9
HAT	histone acetyltransferase
HDAC	histone deacetylace
HILS1	histone H1-like protein in spermatids
HKMT	histone methyl lysine transferases
HMT	histone methyltransferase
HP1	heterochromatin protein 1
JHDM2A	JmjC-domain-containing histone demethylase 2A
K	lysine
LAF	laminar air flow
LSD1	lysine-specific demethylase 1
MBD	methyl-binding domain
MeCP2	methyl CpG binding protein 2
MI	meiose I

MII	meiose 2
mRNA	messenger RNA
MSCI	meiotic sex chromosome inactivation
NaCl	natrium clorid
NCCIT cells	undifferentiated human teratocarcinoma cells
Oct4	octamer-binding transcription factor 4
P	proline
PBS	phosphate buffered saline
PcG	polycomb group
PCI	phenol:chloroform:isoamylalcohol (25:24:1)
PCR	polymerase chain reaction
PCS	pachytene spermatocytes
PHD	plant homeo domain
PHF21A	PHD finger protein 21A
PMSF	phenylmethylsulfonyl fluoride
PRC	polycomb repressive complexes
PRM	protamine
q-rtPCR	quantitative polymerase chain reaction
R	Arginines
RCOR1	REST corepressor 1
RNA	Ribonucleic Acid
RS	round spermatids
RT	room temperature
RT-PCR	Reverse transcriptase
S	serines
SCs	synaptonemal complexes
SDS	sodium dodecyl sulfate
SET	Su(var), Enhancer of zest, and Trithorax.
Sox2	SRY (Sex Determining Region Y) Box-2
Suv39	suppressor of variegation 3-9
T	threonines
TH2B	testis-specific histone H2B
TNP	transition nuclear protein
UTR	untranslated region
UV	ultra violet
Å	Ångstrøm

Table of Contents

1 INTRODUCTION

1.1 Organization of the genome

Nuclear DNA in eukaryotes is linear and organized into chromosomes, each packaged into a compact structure called chromatin. The fundamental unit of chromatin is a structure called nucleosome (Fig. 1a). A nucleosome consists of 145-147 base pairs (bp) of DNA [2] wrapped around two copies of the core histones; histone 2A (H2A), H2B, H3 and H4. The nucleosome is linked together by a stretch of 10-80 bp of linker DNA that is usually associated with histone H1 in higher eukaryotes. Histones are involved in regulating many cellular events such as transcription, DNA replication, recombination and repair. They primarily act either to ensure tight DNA packaging making DNA largely inaccessible, or to relax the chromatin structure making the chromatin less compact and the DNA more accessible [3].

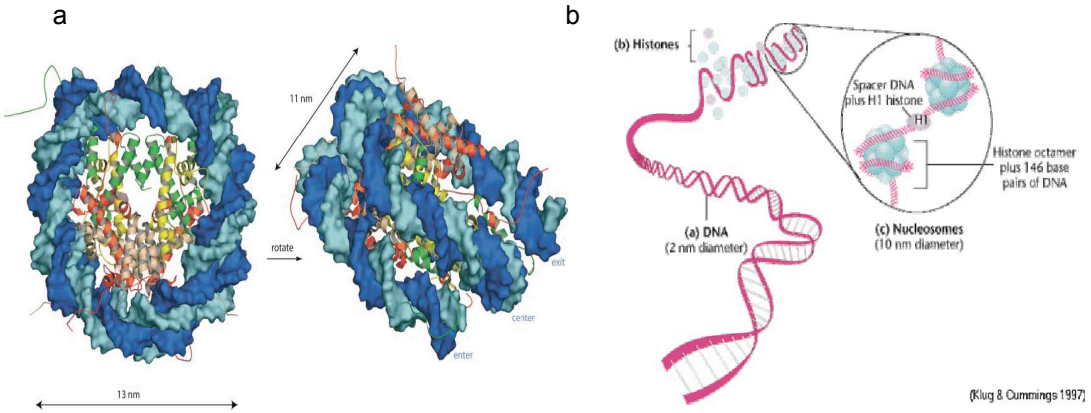

Figure 1: **a)** The atomic structure of the nucleosome. The two DNA strands are shown in pale and dark blue, completing 1.65 turns around an octamer of core histones to make a nucleosome particle with a disc-like structure. Histone H2A is colored in red, H2B in pink, H3 in green and H4 in yellow. From *Khorasanizadeh, 2004*. **b)** Organization of chromatin in the interphase nucleus. The DNA double helix wraps around an octamer of core histones to form a nucleosome. Nucleosomes are spaced by linker DNA which harbors the linker histone H1. From *Klug and Cummings, 1997.*

Chromatin (Fig. 1b) is a dynamic structure and the density of chromatin packaging varies throughout the cell cycle. In general chromatin can be classified into two major forms; active euchromatin and silenced heterochromatin. Active euchromatin is found in the gene-rich transcriptionally active portion of the genome, where DNA is bound

loosely to histones [4]. In silenced heterochromatin, DNA and histones are tightly associated [4], and the genes within it is repressed. Heterochromatin can further be classified as facultative heterochromatin, rich in non-coding repetitive DNA sequences and constitutive heterochromatin which is euchromatin being packaged and repressed during cellular development [5].

The number of protein encoding genes in human are to date estimated to 20,000-25,000. Protein coding genes consist of one or more exons interspersed between introns that is non-protein coding sequences, and at their 5`and 3`ends they have untranslated regions (UTRs) [6]. A proximal promoter that facilitate transcription is located upstream of the transcriptional start site and additional regulatory sequences may be found up- or downstream of the gene [7].

Transcription of protein encoding genes is carried out by RNA polymerase II that needs co-activators to get access to the DNA template. The co-activators may be histone-modifying enzymes that marks chromatin for activation by covalent coupling of chemical groups, such as acetyl or methyl groups to amino acids on NH_2-terminal histone tails [3]. These marks can recruit ATP-dependent chromatin remodeling enzymes that further alter nucleosome conformation to provide an accessible DNA template [8]. Conversely, compaction of chromatin make genes inaccessible for transcription by combined action of co-repressors. By directly binding to DNA or regulatory elements, transcription factors can act as repressors or activators and thus impart to time-, cell- and tissue- specifity of transcription [9].

Many genes encode RNAs that are not translated into protein. Among others are a diverse group of small RNAs involved in regulating mRNA stability, transcription, genome integrity and chromatin structure, and some of them are shown to have important roles in the formation of condensed chromatin [10-12].

1.2 Epigenetic modifications

Epigenetics can be defined as the study of heritable changes in gene expression or cellular phenotype that arises without changes in the DNA sequence [1]. Epigenetic mechanisms such as post-translational histone modifications, DNA methylation, ATP-dependent chromatin remodeling or exchange of histones and histone variants [13] influence the connection between DNA and histones leading to transcriptionally

active or inactive genes [14] and thus these mechanisms are involved in regulating gene expression.

1.2.1 Post-translational histone modifications

Core histones are small basic proteins and consist of a globular domain and a flexible histone tail that protrudes from the nucleosome [4]. Histones possess a large number of modified residues (Fig. 2), especially in their N-terminal tail [15]. These modifications include acetylation, methylation, ubiquitylation and sumoylation of lysine (K) residues; methylation and deamination of arginines (R); phosphorylation of serines (S) and threonines (T); ADP ribosylation of glutamates (E), and proline (P) isomerization [15]. These modified residues may affect chromatin structure by altering inter- and intra-nucleosomal interactions and/or recruit non-histone proteins [16]. The histone modifications can physically directly influence chromatin structure or they can regulate recruitment of proteins onto DNA (nucleosome-remodelling enzymes, transcription factors, histone-modifying enzymes and heterochromatin-associated proteins).

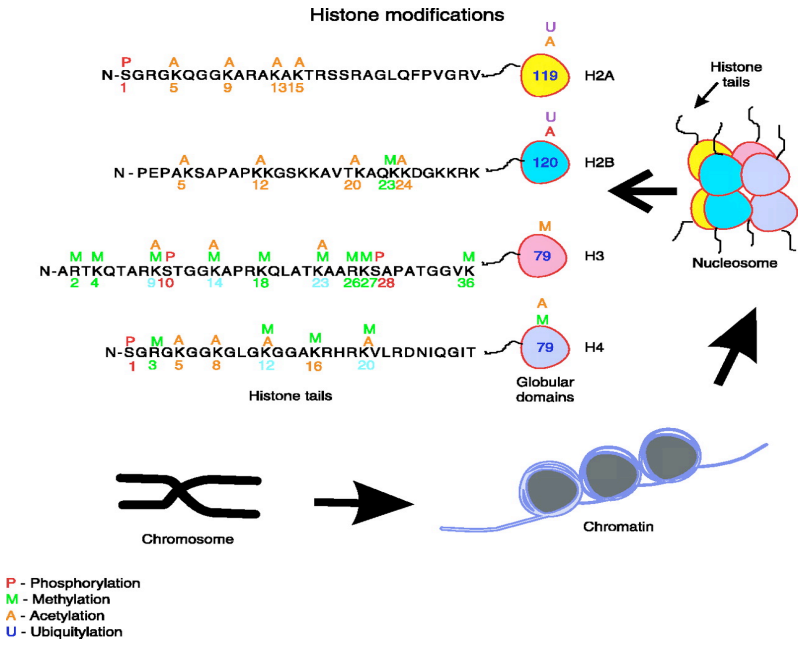

Figure 2: Histone modifications. Some arginine residues (R) can be methylated. Some lysine residues (K) can be either acetylated, methylated or ubiquitylated. Some serine residues (S) can be phosphorylated. From Zamudio N M et al. 2008 [14]

The acetylation of lysines is mediated by histone acetyltransferases (HATs) and acetylated lysines are deacetylated by histone deacetylaces (HDACs). The HATs catalyse the transfer of an acetyl group to the ε-amino group of lysine side chains and thus neutralize the basic charge of the lysines [17]. This leads to weakened interaction between histones and DNA, and by this histone acetylation is generally associated with transcriptionally active chromatin. Deacetylation by HDACs reverses lysine acetylation and is associated with gene repression [14, 17]. This is an example of how histone modifications directly influence chromatin structure, but histone acetylation may also regulate recruitment of proteins onto DNA.

Histone phosphorylation is mostly related to transcriptional activation and takes place on several residues of all the histones. Phosphorylation may also lead to gene silencing, for instance phosphorylation of H2AX forming γ-H2AX during meiosis [18].

One of the most common histone modifications is methylation which mainly occurs on the side chains of lysines and arginines [14, 17]. Lysine residues may be mono-, di- and trimethylated. Arginines have the ability to be mono-methylated or dimethylated either symmetrically or asymmetrically [19]. Histone methylation does not change the charge of the histone protein, instead it function in regulating recruitment of effector proteins that elicit functional outcome. The effector proteins can bind to methylated residues via conserved domains, and methylation is recognized by chromo-like (chromo, tudor) domain and Plant Homeo Domain (PHD). Histone methyltransferases mediate histone methylation while histone demethylases remove methyl groups. Depending on the modified residue, histone methylation is involved in both gene activation and silencing. Methylation of lysine 4 of H3 (H3K4) is related to active transcription, while for instance methylated H3 lysine 9 (H3K9) and H3 lysine 27 (H3K27) are bound by Heterochromatin Protein 1 (HP1) and polycomb, respectively and form compact chromatin [20, 21]. The vast majority of histone methyl lysine transferases (HKMTs) methylate lysines within the N-terminal tails, and they share a Su(var), Enhancer of zest, and Trithorax (SET) domain that harbor the enzymatic activity [17, 19]. The first identified lysine demethylase was termed lysine-specific demethylase 1 (LSD1), which uses flavin adenine dinucleotide (FAD) as a co-factor and can de-methylate mono and di methylated lysine substrates. Another class of de-methylases belong to a family which contain a Jumonji-C (Jmjc)

domain that harbor the enzymatic activity. These enzymes can target removal of all three histone lysine methylation states [19].

1.2.2 DNA methylation

DNA methylation is an epigenetic modification that predominantly occurs at the 5-position of a cytosine-phosphate-guanine (CpG) dinucleotide [22]. DNA methylation is performed by a family of proteins named DNA methyltransferases (DNMTs) [23]. Some of the DNMT3s interplay to mediate de novo methylation in mammalian sperm [24], while DNMT1 work as a maintenance enzyme and preserve previously established methylation patterns during DNA replication [25]. DNA methylation is implicated to have functions in tissue-specific gene expression, cell differentiation, development of gametes and developing embryo such as genomic imprinting, X chromosome inactivation, and retrotransposon silencing [26] among others. Mechanistically, a methylated cytosine base can function to affect recruitment of regulatory proteins [20] or it can affect nucleosome positioning by impacting the affinity for core histones. In the former case, the methyl mark can pass on a binding site for methyl-binding domain proteins MBD1, 2, 3, 4 and MeCP2 and thus mediate transcriptional repression [20, 27]. An example is the silencing of transcription when MeCP2 recruit HDAC and H3K9 HMT activities [28].

1.3 Spermatogenesis

The germ line is rapidly being reprogrammed from spermatogonia stem cells to mature spermatozoa and it therefore offers an attractive system for studying reprogramming of epigenetic gene regulation *in vivo*. During spermatogenesis, global changes in the epigenome occur. Spermatogenesis (Fig. 3) constitute of three major steps: pre-meiotic, meiotic and post-meiotic [29]. Spermatogonia are derived from primordial germ cells that during fetal life were specified to give rise to the germline [30]. The diploid spermatogonia divides mitotically to ensure a generation of self-renewing spermatogonia and to produce primary diploid spermatocytes [29]. Primary diploid (2N) spermatocytes enter the first meiotic division to yield two secondary spermatocytes that are haploid (N). The secondary spermatocytes undergo a second meiotic division to end up with four haploid spermatids [31]. Further post-meiotic

round spermatids develop into mature spermatozoa through a metamorphic process [32].

Developing primary spermatocytes spend over 90% of the time for meiosis in prophase 1 [33]. Prophase 1 can be divided into four stages: leptotene, zygotene, pachytene and diplotene. In the leptotene stage chromosomes start condensing and double-strand breaks (DSBs) that are essential for homologous recombination start to form [34]. During the zygotene stage, sister chromatids pair and synaptonemal complexes (SCs) that are proteinaceous structures are formed [35]. The SYCP3 protein is a component in the SCs. At the pachytene stage synapsis is completed and homologous recombination occurs. In the diplotene stage the synaptonemal complex breaks down and the chromosome separation is initiated [36].

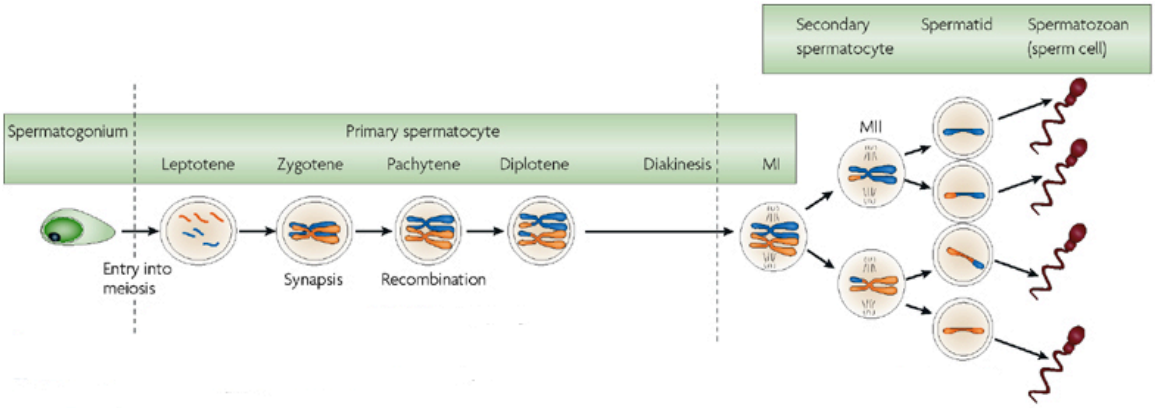

Figure 3: The development from spermatogonium to mature spermatozoan (spermatid) through spermatogenesis. MI, meiose I; MII, meiose 2. Adapted and modified from *Sasaki et al. 2008* [37]

1.3.1 Epigenetic regulation of genes critical to mammalian spermatogenesis

Spermatogenesis, the differentiation of male primordial germ cell to mature spermatozoa, requires specific and comprehensive chromatin and epigenetic remodeling [38]. The timing of establishment and removal of methylation marks is critical for completing normal spermatogensis, [39] and factors that control histone methylation are substantial. In this context the lysine specific histone methyl transferases (HMTases) are important players such as the HMTases SUV39H1 and SUV39H2 [40]. SUV39H1 and SUV39H2 carries out trimethylation of H3K9 at pericentric heterochromatic regions [14]. Methylation of H3K9 results in a high-affinity binding site for heterochromatin protein 1 (HP1) proteins [41]. *Suv39h2* is

mainly expressed in testis [42]. In *Suv39h2* deficient mice, pachytene spermatocytes undergo apoptosis due to incomplete pairing and synapsis. This indicates an essential role in the mouse germ cell lineage [40]. Another important HMTase G9a, which is claimed to be the major mammalian H3K9 mono- and dimethyltransferase [43] has also been proven to be important in male meiosis. Loss of *G9a* affected spermatocytes which failed to develop past the pachytene stage and thus *G9a* knockout mice were sterile [44]. MEISETZ (also known as PRDM1) is a histone methyltransferase that mediates H3K4 trimethylation and is arrogated to be necessary for proper meiotic prophase progression [45]. Loss of *Meisetz* leads to deficient pairing of homologous chromososmes, meiotic arrest and sterility [45].

Histone methylation can be reversed by histone demethylases. KDM1 (also known as Aof2 or LSD1) is a histone demethylase that demethylates mono and dimethylated H3K4 and function in complex with histone deacetylases HDAC1/2, REST corepressor 1 (RCOR1) and PHD finger protein 21A (PHF21A) to repress transcription [46]. A tightly regulated distribution of KDM1 is presented during spermatogenesis [46]. KDM1b a histone H3 lysine 4 demethylase related to KDM1, is important for establishing the DNA methylation imprints during oogenesis [47].

JHDM2A (JmjC-domain-containing histone demethylase 2A) is necessary for spermatogenesis, it is expressed during and after meiosis from the late pachytene stage until the elongated spermatid stage, with its highest level in round spermatids [48]. JHDM2A helps to regulate the expression of the spermatid-specific proteins transition nuclear protein 1 (TNP1) and protamine 1 (PRM1) by demethylating mono- and di- methylated H3K9 in the promoter regions of these proteins [48]. In a study by Okada et al. [48] it was found that mice deficient for *Jhdm2a* possess post-meiotic chromatin condensation defects.

1.3.2 Post-meiotic remodeling

Elongating spermatides undergo a process called the histone-to-protamine transition that prepare these cells for fertilization [49]. In this process histones are replaced with transition nuclear proteins (TNP1 and TNP2) followed by the replacement of these proteins with protamines (PRM1 and PRM2) [48] resulting in a denser DNA packaging in sperm. The nuclear transition proteins are thought to prepare the chromatin for association with protamines by affecting DNA condensation [48].

Protamines are only found in spermatids [50], they are small and basic proteins and more than 50% of their residues are arginine resulting in high DNA binding affinity [49]. Not all histones are replaced by protamines in mature (human) sperm. Rare retained nucleosomes with either canonical histones or histone variants exist [51]. In a study where nucleosomes retained in mature spermatozoa were mapped, histone retention was found at loci important for embryo development, and promoters of both micro RNA and imprinted genes [51, 52].

1.3.3 Histone variants involved in spermatogenesis

During spermatogenesis histone variants are incorporated into nucleosomes. Additionally, the degree of chromatin folding is influenced by the linker histone H1, and there are three testis specific H1 variants identified in mammals H1t, H1t2 and HILS. H1t displace the somatic H1A and H1B during meiotic prophase and thus initiates the restructuring of sperm chromatin [53]. H1t2 appears to play a role in directing chromatin condensation [54]. HILS1 (histone H1-like protein in spermatids) is confined to elongating spermatids. It is suggested that HILS1 is linked to chromatin condensation because of the equal nuclear distribution of HILS1, transition protein 2 and protamine 1 [55].

The histone variant H2AX influence chiasmata formation in meiosis because of its function at double-strand breakage sites [56]. H2AX also influence meiotic sex chromosome inactivation (MSCI). MSCI is a process where the X and Y chromosomes form an XY (or sex) body and become transcriptionally silent in the pachytene stage of meiosis [57]. Phosphorylated H2AX (γ-H2AX) localizes to the XY body independently of DSBs occurring [18]. H2AX phosphorylation is dependent on the DNA repair protein ataxia telangiectasia and Rad3 related (ATR) [58] and ATR is dependent on BRCA1 for its recruitment to the XY-body [58]. Thus, H2AX phosphorylation, ATR and BRCA1 act together to initiate MSCI [14].

TH2B (testis-specific histone H2B) is a testis specific variant of the somatic H2B and has an important role in the remodeling of chromatin structures during spermatogenesis [59]. TH2B has a different phosphorylation pattern than H2B because of the addition of three potential phosphorylation sites and repositioning of two others in the N-terminal tail of TH2B [60]. The unequal distribution of TH2B in the nucleus suggest regulation of specific chromatin domains [60]. Furthermore,

TH2B was found in rare retained nucleosomes in human sperm [51]. In a study by Hammoud et al. 2009 [51] where the localization of unmodified histones retained in sperm was examined, it was found that relative high levels of TH2B were present at gene promoters in loci important for sperm biology, capacitation and fertilization, but not at developmental loci [51].

1.4 Maintenance of pluripotency

Spermatogonial stem cells maintain a sufficient population of spermatogonia by regulated proliferation and differentiation but they also need to ensure a generation of self-renewing spermatogonia i.e. some of the spermatogonia need to maintain their stem cell potential. This ability to either self renew or differentiate into specialized cell types is a key feature spermatogonia have in common with other types of stem cells such as hematopoietic stem cells and embryonic stem cells. Embryonic stem cells are the most thoroughly studied cell type when it comes to the involvement of chromatin and epigenetic factors in the regulation of stem cell potential and differentiation.

In order to maintain a pluripotent state of embryonic stem cells (ES cells), pluripotency genes need to be expressed while lineage genes need to be silenced. At the same time it is important that lineage genes are rapidly induced upon differentiation. Histone modifications play an important role in this regulation. *Oct4* (also known as *Pouf1*) and *Nanog* are transcription factors that need to be expressed in ES cells and the early embryo to achieve pluripotency [13]. Embryonic stem cells (ES cells) are characterized by a specific epigenetic profile [61] where lineage specific genes are kept in a state where they are inactive but have the potential for activation upon differentiation. This is achieved through the bivalent marking with H3K4me3, a mark of active genes, and H3K27me3, a mark of inactive genes at genes encoding transcription factors that are important in embryonic development and lineage specification [61, 62]. Genes with bivalent marks (Fig. 4) show low-level transcription or are silenced in ES cells, and are believed to be poised for transcriptional activation upon differentiation. Upon differentiation bivalent ES cell domains are for the most part resolved into containing either H3K4me3 or H3K27me3 [63] and depending on the particular role of the gene and the developmental direction they become either activated or repressed [61]. Worth to

mention is that one-third of all genes have neither modifications which suggest the presence of other epigenetic markers function to maintain a pluripotent genome [64, 65]. The role of bivalent marks in the haploid life cycle, i.e. spermatogenesis, has yet to be explored/established.

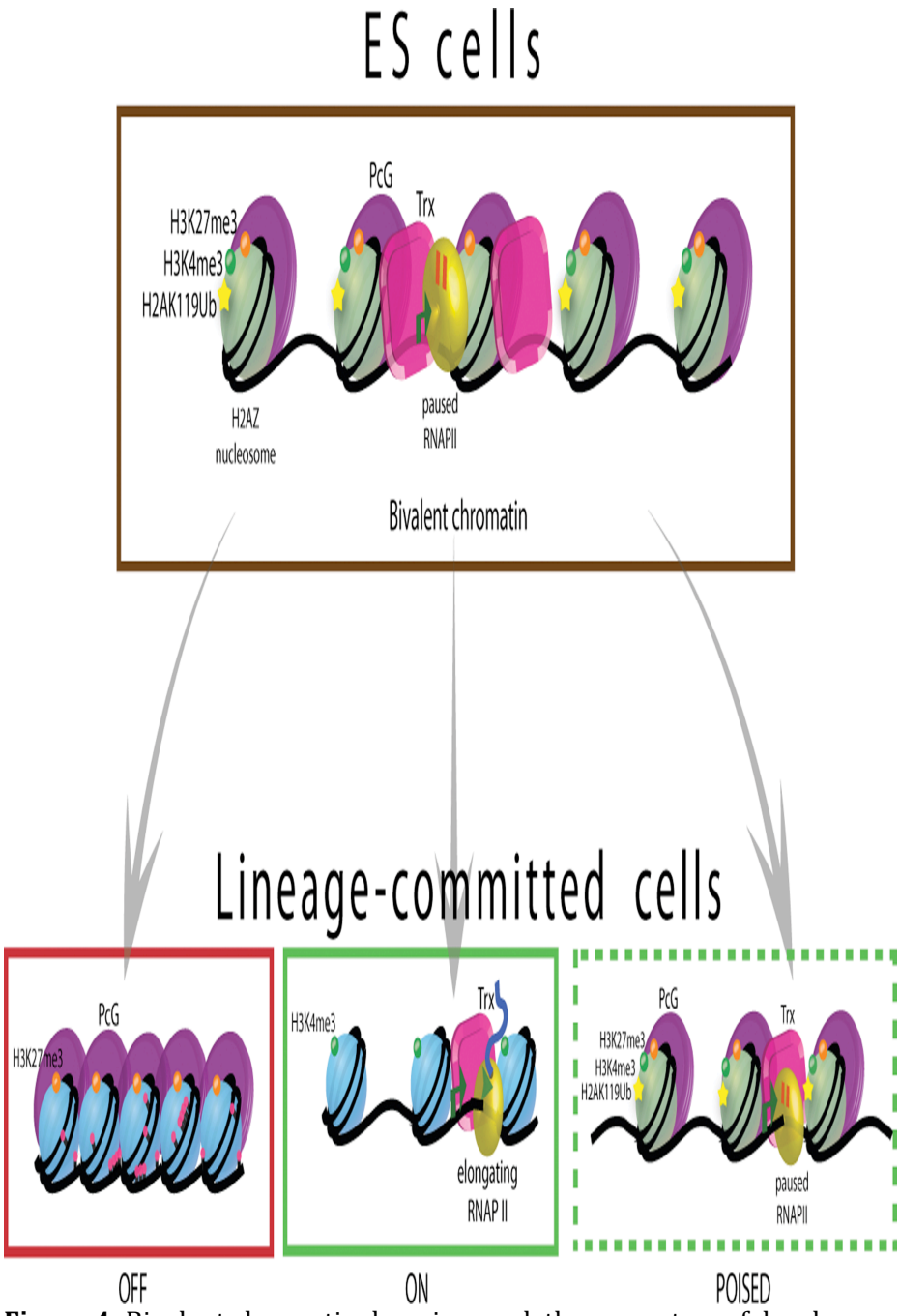

Figure 4: Bivalent chromatin domains mark the promoters of developmentally important genes in pluripotent ES cells. PRC2 and TrxG proteins catalyze the tri-methylation of histone H3 on lysine 27 and 4, respectively. Genes with bivalent marks show low-level transcription or are silenced, and are believed to be poised for transcriptionally activation upon differentiation. Upon differentiation, the bivalent histone marks can be resolved to monovalent modifications in which the gene is "ON" or "OFF". Bivalent domains can also be maintained or newly established in lineage-committed cells. From *http://www.stembook.org/node/585*

1.5 Analysis of histone modifications by chromatin immunoprecipitation (ChIP)

Chromatin immunoprecipitation is an analytical method for investigating nuclear proteins-DNA interactions inside the cell [66, 67] and it involves immunoprecipitation of protein/DNA complexes. The concept of ChIP is outlined in figure 5. In brief, DNA-binding proteins are reversibly cross-linked to DNA with formaldehyde which can cross-link components within a distance of 2 Å [68]. To release the chromatin from the cell nucleus, the cross-linked cells are lysed. Next, the chromatin is sheared by sonication to generate chromatin fragments of about 200-1000 bp, with e.g. an average of 500 bp. The lysate is cleared by sedimentation and the protein of interest is immunoprecipitated using specific antibodies recognizing, for instance as in this study, histone modifications or histone variants. To remove non-specific bound chromatin the immunoprecipitated complexes are washed under stringent conditions. The precipitated chromatin is eluted, cross-links are reversed, proteins are digested and the precipitated ChIP-enriched DNA is purified [66]. DNA sequences associated with the precipitated protein can be identified by end-point polymerase reaction (PCR), quantitative (q) PCR, labeling and hybridization to DNA microarrays or direct high-throughput sequencing (ChIP-seq) [66].

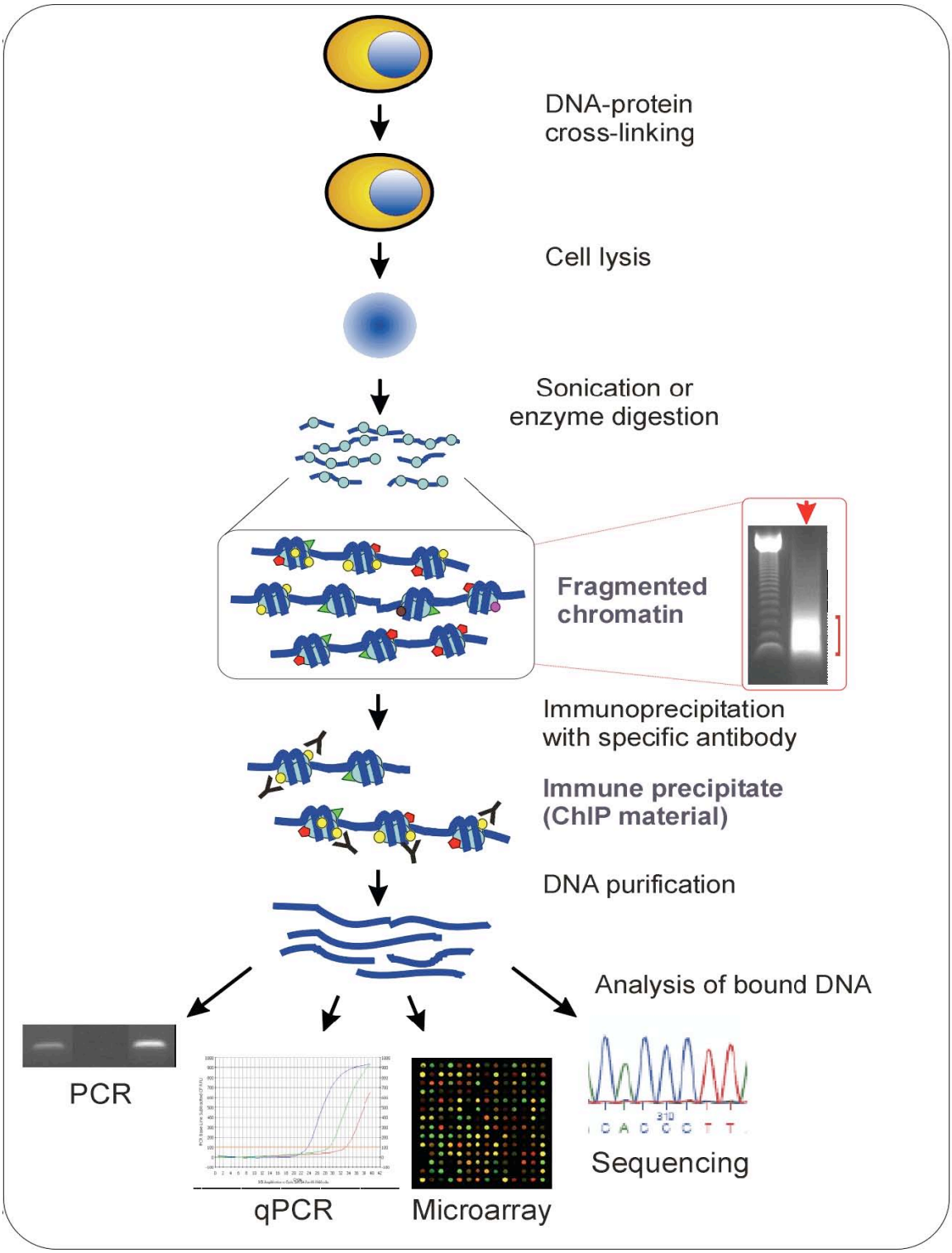

Figure 5: The chromatin immunoprecipitation (ChIP) assay. DNA sequences associated with the precipitated protein can be identified by end-point PCR and elechtrophorese, qPCR, labeling and hybridization to DNA microarrays or sequencing. From *Collas and Dahl 2008 [69]*.

2 MATERIALS

2.1 Chemicals

Table 1: Chemicals used in this study

Name (Company, Catalog number)
0,1 % SDS (Sigma-Aldrich, L4509)
0,1 %sodium deoxycholate (Sigma-Aldrich, D5760)
1% TX-100 (Sigma-Aldrich, T8787)
250 mM EGTA (Sigma-Aldrich, T3253)
36.5% Formaldehyde (Sigma-Aldrich, F8775)
5 M NaCl (Sigma-Aldrich, S5150)
6x loading buffer (Fermentas, R0611)
70% (vol/vol) Ethanol
96% (vol/vol) Ethanol
Acrylamide carrier (Sigma-Aldrich, A9099)
Cell Adherence Solution (Crystalgen, 301-025-015)
Chloroform:Isoamylalcohol, 24:1 (Sigma-Aldrich C0549-1PT)
Collagenase type IV (Gibco, 17104-019)
DAPI (4',6-diamidino-2-phenylindole, dihydrochloride) (Invitrogen, D1306)
Deoxyribonuclease I from bovine pancreas, DNAse (Sigma Aldrich, DNEP)
DMEM/F12 (Invitrogen, 11320-074)
Dynabeads Protein A beads (Invitrogen, 100-020D)
EDTA (Sigma-Aldrich, E5134)
Formaldehyde (Sigma-Aldrich, F8775)
GeneRuler DNA ladder mix (Fermentas, SM0331)
Glycine, Sigma-Aldrich G8790
Goat serum (DAKO x0907)
High Capacity cDNA Reverse Transcription Kit (Applied Biosystems, 4368814)
Hyaluronidase (Sigma, H6254)
Lysing Matrix D (Medinor / MP Biomedicals, 6913-050)
PBS (Sigma-Aldrich, P4417)
Penicillin-Streptomycin, Pen Strep (Invitrogen, 15070-063)
Phenol-chloroform-isoamylalcohol 25:24:1v/v (Invitrogen, 15593-031)
Phenylmethylsulphonyl fluoride, PMSF (Sigma-Aldrich, P7626)
Phosphate buffered saline (Sigma, p4417)
Polyacryl-carrier (Molecuar Research Center, Inc PC 152)
Power SYBR green master mix (Applied Biosystems, 4368702)
Protease inhibitor mix (Sigma-Aldrich, P8340)
Proteinase K (Sigma-Aldrich, P2308)
Qubit™ dsDNA HS assay kit (Invitrogen Q32851)
RNAzol RT reagent (Molecuar Research Center, Inc RN 190)
Sodium acetate, NaAc (Sigma-Aldrich C8750)
Sodium Butyrate, Na-butyrate (Sigma-Aldrich, B5887)

SYBR® Safe DNA Gel Stain (Invitrogen, S33102)
Tris-HCl (Sigma-aldrich, T3253)
Triton X-100 (Sigma-Aldrich T8787)
Trypsin from bovine pancreas (Sigma-Aldrich, T1426-50MG)
TURBO DNA-free KIT (Applied Biosystems, AM1907)
Tween 20 (Sigma-Aldrich, P2287)
Ultrapure agarose (Invitrogen, 16500100)
UltraPure™ Phenol:Chloroform:Isoamyl Alcohol, 25:24:1, v/v (Invitrogen, 15593-031)

2.2 Antibodies

Table 2: Antibodies used in immunofluorescence staining

Antibodies	**Company, Catalog number**
Anti-phospho-Histone, H2AX	MedProbe / Upstate Biotechnology, 05-636
Anti-SCP3 antibody	Abcam ,ab15092
Lectin PNA, Alexa Fluor 594 conjugated	Invitrogen, L-32459
Alexa Fluor 488 Goat Anti-Mouse IgG	Invitrogen, A-11029
Alexa Fluor 594 Donkey Anti-Rabbit IgG	Invitrogen, A-21207

Table 3: Antibodies used for Chromatin immunoprecipitation

Antibodies	**Company, Catalog number**
TH2B	Upstate,Millipore, 07-680
H3K4me3	Diagenode, pAb 003-050
H3K9me2	Diagenode, mAb-154-050
H3K9me2	Diagenode, pAb-060-050
H3K27me3	Diagenode, mAb-181-050
H3K27me3	Diagenode, pAb-069-050
H3K27me3	Millipore, CS200603

2.3 Buffers

Table 4: Buffers used in this study

Name	Contents
ChiP complete-elution buffer	20 mM Tris-HCL, pH7.5, 5mM EDTA, 50 mM NaCl, 20mM Na-butyrate, 1% (wt/vol) SDS, 50ug ml-1proteinase K
ChIP-elution buffer	20 mM Tris-HCL, pH7.5, 5mM EDTA, 50 mM NaCl, 20mM Na-butyrate
Lysis buffer	50 mM Tris–HCl, pH 8, 10 mM EDTA, 1% (wt/vol) SDS, protease inhibitor cocktail (1:100 dilution from stock), 1 mM PMSF
RIPA buffer	10 mM Tris–HCl, pH 7.5, 140 mM NaCl, 1 mM EDTA, 0,5mM EGTA, 1% (vol/vol)Triton X-100, 0.1% (wt/vol) SDS, 0.1% wt/vol) sodium-deoxycholate,)
RIPA ChIP buffer	10 mM Tris–HCl, pH 7.5, 140 mM NaCl , 1 mM EDTA, 0,5mM EGTA, 1% (vol/vol)Triton X-100, .1% (wt/vol) SDS, 0.1% wt/vol)Sodium-deoxycholate, protease inhibitor mix(1:100 dilution from stock)
TE-buffer	10mM Tris-HCL, pH 8,0, 1mM EDTA

3 Methods

3.1 Cell Culture and Germ Cell isolation

In this study undifferentiated human teratocarcinoma cells NCCIT (CRL-2073) obtained from American Type Culture Collection (ATTC) and pachytene spermatocytes and round spermatids cells isolated from C57/BL6 mice were used.

3.1.1 Cell culture of NCCIT cells

Cell culture work was performed in laminar air flow hoods (LAF-hood) using sterile techniques. The NCCIT cells were cultured in RPMI 1640 medium and grown in sterile Nuclon screw cap flasks, T-75 (cm of surface area) and incubated at 37 °C with the ambient air containing 5% v/v CO2. Maintenance of the cells consisted of removing the confluent cultures (densely grown cells) from the flask and passaging into another flask at a lower density. To perform this subculturing the medium was removed from the cells attached to the bottom of the flask. Fresh medium was added, and the cells dispersed by agitation (by hitting the flask against the palm of one hand). Finally, the cells were observed under a microscope. The cells were subcultured twice a week.

3.1.2 Separation of germ cells

Pachytene spermatocytes (PCS) and round spermatids (RS) were isolated from sexually mature C57/BL6 wild type mice testes using the STA-PUT technique. Cells that differ in size, shape and volume have different sedimentation velocity. The STA-PUT technique utilizes the differential sedimentation velocity at unit gravity to separate cells [70, 71]. First a suspension of free germ cells was isolated from the testes through washes and enzymatic digestions and then germ cells was separated by the STA-PUT apparatus. The separation of germ cells was carried out as described by *Ravindranath et al. 1999* [70] with modifications.

Preparation of cell suspension

Procedure:

1) Under sterile conditions, testes from six C57/BL6 wild type mice were removed from the abdominal cavity and put in Dulbecco's Modified Eagle Medium/F12 (DMEM/F12) supplemented with antibiotics (100x penicillin and streptomycin)
2) Testes were then placed on a petri dish in a small quantity of DMEM/F12.
3) To excise and decapsulate the testes, an incision was made in the tunica albuginea and the contents were pulled out using tweezers.
4) The detunicated testes were transferred to a 50 ml tube containing ice cold DMEM/F12, allowed to sediment, and washed 3 times in DMEM/F12 by pouring 15 ml of DMEM/F12 into the tube, mixing gently, letting the testes sediment and removing the DMEM/F12 by a glass-pipette.
5) After the last wash most of the media was removed, and the detunicated testes were poured back into the petri dish and minced into small pieces with a pair of scissors. This was done for about five min until a homogeneous medium was obtained.
6) The minced tissue was pipetted back into a 50 ml tube. To be sure of getting all of the minced tissue, the petri dish was rinsed with a small volume of DMEM.
7) The minced tissue containing connective tissue, somatic cells and seminiferous tubules were washed twice in DMEM/F12 by pouring 15 ml of DMEM/F12 into the tube, mixing gently, letting the cells sediment for 5 min and removing the DMEM/F12 by a glass-pipette leaving 5 ml in the tube. After the last wash most of the DMEM/F12 was removed.
8) To break down connective tissue and somatic cells, an enzyme mix consisting of 10 ml DMEM/F12, 1 mg/ml collagenase type IV and 1 µg /ml DNAse were added, mixed and incubated for 8 min at 34 °C on rotation.
9) After incubation, a glass-pipette was used to help release tubules by pipetting up and down several times. A drop of the suspension was placed on a microscope slide and checked under a phase contrast microscope. It was expected to see long tubules surrounded by interstitial cells. Before removing the enzyme-mix, the tubules were allowed to sediment for 5 min

10) To remove interstitial cells, tubules were washed 5 times by pouring 15 ml of DMEM/F12 into the tube, mixing gently, letting the testes sediment for 5 min, and then remove the DMEM/F12 by a glass-pipette. About 2-3 ml of the media was allowed to remain between every wash. After the last wash most of the media was removed.
11) In order to break down the tubules and release germ cells, an enzyme mix consisting of 10 ml DMEM/F12 with 1 mg/ml collagenase type IV, 1,5 mg/ml hyaluronidase, 1mg/ml trypsin and 20 ul DNAse (1µg/ml) were added, mixed and incubated for 15 min at 34 °C on rotation. After the incubation, a glass-pipette was used to break apart the tubules by pipetting up and down several times. The cell suspension was then checked under a microscope and it was expected to see only free germ cells and no tubules. If tubules were still present, the cell suspension was incubated for another 2-3 min at 34 °C on rotation and repeated pipetting after that.
12) The cell suspension was then poured into a fresh 50 ml tube, resuspended in 10 ml DMEM/F12 with 0,5% BSA and centrifuged 300g for 10 min at 10°C.
13) After centrifugation, the supernatant was discarded and the cell pellet was resuspended gradually by 25 ml of DMEM/F12 with 0.5% BSA and 20 µl DNAse. The cells were counted in a Countess® Automated Cell Counter (Invitrogen). Expected yield were 1-4x10^6 cells per ml. The cell suspension was then filtered through two cell strainers (70 µm nylon mesh) to remove cell aggregates and finally the cells were ready for the STA-PUT apparatus.

3.1.3 STA-PUT apparatus

The STA-PUT apparatus was used to separate germ cells by sedimentation velocity at unit gravity at 4 ^{o}C by a 2-4% BSA gradient in DMEM/F12. The STA-PUT apparatus is illustrated in figure 6.

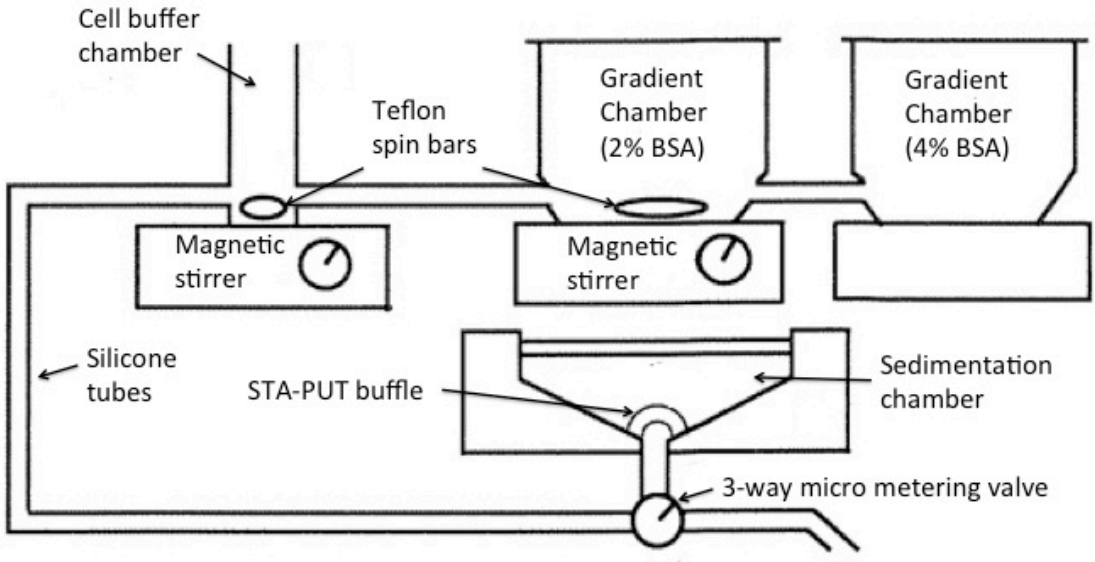

Figure 6: The STA-PUT apparatus consist of two gradient chambers, a cell buffer chamber, two magnetic stirrers, two teflon spin bars, a sedimentation chamber with a STA-PUT buffle and a 3-way micro metering valve. Silicone tubes connect the gradient chambers, cell buffer chamber and the sedimentation chamber to each other. The figure is modified from http://www.tecniglas.com/images/STA-PUT.2008.Cdn.Information.pdf.

Procedure:

1) All connecting tubes were saturated with DMEM/F12 and all air bubbles were removed.
2) The valves were closed and the tubing between the gradient chambers clamped.
3) The two gradient chambers were filled with 550 ml DMEM/F12 with 2% BSA and 550 ml DMEM/F12 with 4% BSA.
4) 50 ml of DMEM/F12 with 0.5% BSA was added to the cell loading chamber and allowed to enter the sedimentation chamber.
5) Then the cell suspension was loaded into the cell buffer chamber, the magnetic stirrer was set on, and the cell solution was allowed to go into the sedimentation chamber. This was supposed to take about 10 min.

6) After the cell suspension was loaded into the sedimentation chamber, the magnetic stirrer under the 2% BSA solution was set on, clamps were removed and the 2-4% BSA gradient was introduced slowly under the cell suspension, displacing the cells to form a thin band near the top of the chamber [72]. The gradient was made to stabilize against convection and prevent mixing of adjacent layers during loading and unloading of the sedimentation chamber [72, 73].
7) After approximately 30 min, the valves were closed and the cells were allowed to sediment for 2.5 hrs.
8) After sedimentation, 10 ml fractions were collected and centrifuged at 1000 rpm for 10 min at 10°C. Then the volume of the fractions was reduced to 1 ml.
9) Fractions containing pachytene spermatocytes (12-18 μm) and round spermatids (8-10 μm) were selected by looking at the cell size and morphology using a phase contrast microscope and a Countess® Automated Cell Counter.
10) Fractions containing the same cell type, PCS or RS, were pooled to obtain cell populations enriched in PCS or RS, spun down at 1000 rpm for 10 min at 10°C. Supernatant was discarded and the cells were resuspended in 1 ml of PBS. Then cells were counted in a Countess® Automated Cell Counter.
11) For microscopic analysis of purity, an aliquot of isolated pachytene and round spermatids was fixed on SuperFrost Plus slides (VWR) using Cell Adherence Solution, and stored in -20°C freezer.

3.1.4 Animal handling

Mice were kept under controlled photoperiod conditions (light from 07:00–20:00 h) and were supplied with commercial feed and tap water *ad libitum*. Mice were anesthetized with isoflurane and killed by cervical dislocation. All experiments and procedures involving the use of animals in research were approved by the Section for Comparative Medicine at Oslo University Hospital and by the Norwegian Animal Research Authority, complied with national laws and institutional regulations and followed the guideline by Federation for Laboratory Animal Science Associations (FELASA).

3.2 Immunofluorescence staining of pachytene and round spermatids.

To asses the purity of the pachytene and round spermatids cells, an aliquot of the isolated cells were spread on SuperFrost Plus slides (VWR) and stained with fluorescent dyes using antibodies against proteins found in the cells. The pachytene spermatocytes were stained with the primary unconjugated antibodies anti-phospho-Histone H2AX and anti-SCP3 antibody, and the secondary antibodies Alexa Fluor 488 Goat Anti-Mouse IgG, and Alexa Fluor 594 Donkey Anti-Rabbit IgG. Round spermatids were stained with Lectin PNA From *Arachis hypogaea* (peanut), Alexa Fluor® 594 Conjugated. In addition both cell types were counterstained with DAPI (4',6-diamidino-2-phenylindole, dihydrochloride) that stained the DNA blue.

Procedure:

1) Slides were washed quickly in phosphate buffered saline (PBS) and fixated in 4% paraformaldehyde (PFA) in PBS for 10 min at room temperature (R.T) in a fume hood. After fixation the slides were washed twice in PBS for 5 min.
2) To permeabilize the cells, PBS with 0,5 Triton X-100 was added to the slides and incubated for 5 min followed by two washes in PBS.
3) In order to reduce background staining, the slides were incubated in a blocking solution (PBS with 0,1% tween, 5% bovine serum albumin (BSA) and 5% goat serum), for 30 min at R.T.
4) After blocking, slides with pachytene spermatocytes were incubated with the primary antibodies namely anti-phospho-histone H2AX and anti-SCP3 diluted in antibody diluent solution (PBS with 0,1% tween, 0,5% BSA and 0,5% goat serum). The two antibodies were mixed in one solution and thus incubated simultaneously. The round spermatids were incubated with diluted conjugated PNA. The incubation was carried out in an incubation box at 4°C over night.
5) To remove unbound primary antibody the slides were washed 3x10 min in PBS-tween, and then incubated with the secondary antibody diluted in antibody diluent solution (1:500 for both antibodies) for 30 min followed by three washes in PBS-tween for 10 min.
6) Cells were counterstained with DAPI (the DAPI stock solution (5mg/ml) was diluted 1:5000 in PBS) for 5 min and washed 3x10 min in PBS.
7) After the last wash, most of the water was removed from the slides and a drop

of the mounting medium Mowiol and a coverslip was added. The mounted slides were dried for 2 hrs before they were examined under an Axio Observer.Z1 microscope. The minimum numbers of cells examined was hundred.

3.3 Chromatin immunoprecipitation (ChIP)

In this thesis, ChIP was performed with anti-histone antibodies specific for H3K4me3 on chromatin from NCCIT cells and antibodies specific for TH2B, H3K4me3, H3K9me2 and H3K27me3 on chromatin from pachytene spermatocytes and round spermatids. In general ChiP was performed as described previously in the protocol *A rapid micro chromatin immunoprecipitation assay, Dahl at al. 2008* [66] with modifications.

3.3.1 ChIP on NCCIT cells

Preparation of Antibody-bead complexes:
In order to immunoprecipitate chromatin, magnetic beads were loaded with antibodies specific for H3K4me3.

Procedure:

1) 100 µl of well-suspended Dynabeads Protein A beads were placed into a 1,5-ml eppendorf tube, washed twice in 400 µl RIPA buffer, and resuspended in 90 µl of the same buffer.
2) 90 µl RIPA buffer was aliquoted into 200 µl PCR tubes, one tube per chip. 10 µl of beads and 4 µl of the antibody H3K4me3 (cat# pAb-060-050, Diagenode) were added to each tube, the ChIP was performed in triplicate. A triplicate of negative controls, (No-antibody control) were also prepared by adding the same amount of RIPA buffer and beads into each tube, except the antibody.
3) The antibody-bead complexes were incubated on a rotator at 4^{o}C for at least 2 hrs.

Cross-linking of DNA and proteins

In order to maintain the association of proteins with their target DNA sequence inside the NCCIT cells, formaldehyde was used to reversibly cross-link proteins to DNA. Glycine was added to quench the formaldehyde and terminate the cross-linking reaction.

Procedure

1) 270 µl 36,5% formaldehyde was added to NCCIT cells solved in 10 ml phosphate buffered saline (PBS), mixed by gentle vortexing and incubated for 8 min at room temp (R.T)
2) The cross-linking was quenched for 5 min at room temp by adding 1140 µl glycine. From now on the samples were kept on ice and cold buffers were used except as otherwise stated.
3) The cross-linked cells were centrifuged at 400g for 10 min at 4°C in a swing-out rotor. The supernatant was discarded leaving 30 µl of the solution with the cell pellet.
4) The crosslinked cells were washed twice in 10 ml of ice-cold PBS, by adding PBS, mixed and centrifuged with the same settings as above.
5) After the last wash, the cells were resuspended in 1 ml of PBS and the cellsuspension was removed to a 1,5 ml eppendorf tube. The eppendorf tube was centrifuged as above and the PBS was discarded leaving 20 µl with the cell pellet.
6) The cross linked cell pellet was frozen in liquid nitrogen and stored at -80°C.

Lysis of cells and sonication

To release chromatin from the nucleus, the crosslinked cells were lysed and the cell lysate were sonicated by a Labsonic M sonicator (Labsonic M, Ø3 mm probe, Sartorius) to generate sheared, soluble chromatin fragments of 400-500 base pair.

Procedure:

1) 175 µl lysis buffer (R.T) was added to the cell pellet (35µl), vortexed 2x5 s, left on ice for 5 min and resuspended by vortexing.

2) The cell lysate was then sonicated on ice for 10x30 s, with 30 s pauses on ice between each 30-s session using a Labsonic M pulse sonicator. The pulse settings were: cycle 0.5, 30% power.

3) The sonicated cells were centrifuged at 12,000g for 10 min at 4°C, and 120 µl of the supernatant (chromatin) were transferred into a clean 1.5-ml tube.

Absorbance measurement and dilution of chromatin

To determine the concentration of chromatin an absorbance measurement was done at 260 nm on a Nanodrop ND-1000 Spectrophotometer (NanoDrop Technologies). The chromatin was diluted to 2 A_{260} in RIPA ChIP buffer. 100 µl chromatin with the concentration 2 A_{260} is equivalent to approximately 100 000 NCCIT cells.

Immunoprecipitation and washes

The anti-histone antibody H3K4me3 was used to capture the histone modification H3K4me3 and the interacting DNA. In order to remove non-specific bound chromatin the immune complexes were washed.

Procedure:

1) Tubes with bead-antibody incubation was briefly spun down in a table top centrifuge and placed in a magnetic rack to pellet beads.
2) The supernatant was discarded and the beads were washed once in 100 µl RIPA buffer. The tubes were removed from the magnetic rack to release the beads into the buffer. Then the tubes were briefly vortexed, spun down, placed in the magnetic rack and the RIPA buffer was discarded.
3) 100 µl of fragmented 2U chromatin was added to each tube. The tubes were removed from the magnet, vortexed and incubated on a rotator at 4°C for 2 hrs.

4) For input samples and chromatin fragmentation assessment, 100 µl and 20 µl respectively of fragmented 2U chromatin, were aliquoted into 1,5 ml eppendorf tubes and put on ice. The input samples were run in triplicate.
5) After incubation the tubes were briefly spun down and placed in a magnetic rack to pellet beads. Supernatant was removed and 100 µl RIPA buffer was added. The tubes were removed from the magnetic rack, mixed by vortexing and placed on a rotator for 4 min at 4°C. This washing step was repeated three times in RIPA buffer and once with TE-buffer.
6) To reduce the background noise the samples in TE buffer were transferred into new PCR tubes.

DNA-elution, cross-linking reversal and Proteinase K treatment of the chromatin

Procedure:

1) From now on the samples were kept in room temperature. The samples were placed in a magnetic rack and the TE-buffer was removed.
2) DNA elution (1% SDS), cross-link reversal and protein digestion (proteinase K) were carried out in one step. For this 150 µl ChiP complete-elution buffer was added to the chip-samples. The samples were vortexed and incubated on a thermomixer for 2,5 hours at 68^{o}C, 1300 rpm. For the input samples 200 µl of ChIP-elution buffer and 2µl proteinase K were added, and 180 µl Milli Q (MQ) water and 2µl proteinase K was added to the fragmentation assessment sample. These samples were incubated on a heating block for 2,5 hours at 68°C.
3) The ChIP samples were placed in a magnetic rack and the supernatant containing precipitated chromatin was collected and placed into a clean 1,5 ml eppendorf tube.
4) 150 µl elution buffer was added to the remaining ChIP material and incubated on the thermomixer for 10 min at 60°C, 1300 rpm. The supernatant was collected as in 3) and pooled with the first supernatant.
5) All samples were filled up to 500 µl with ChIP-elution buffer for PCI extraction.

Phenol-chloroform-isoamylalcohol extraction of the precipitated chromatin.

Procedure:

1) 500 µl Phenol-chloroform-isoamylalcohol (25:24:1v/v) was added to each samples, vortexed vigourosly and centrifuged at 15000 g, 5 min at RT to separate the phases. 460 µl of the upper phase containing DNA was collected and transferred to a clean tube.
2) 460 µl of chloroform:isoamylalcohol (24:1) was added, vortexed and centrifuged as above and 400 µl of the upper phase was transferred to a clean tube.
3) From this step the samples were kept on ice. The DNA was precipitated by adding 40 µl NaAc, 10 µl acrylamide carrier and 1 ml ice-cold 96% (vol/vol) ethanol. Then the samples were vortexed thoroughly and incubated over night at -80 °C.
4) The samples were thawed on ice and centrifuged at 20 000g for 10 min at 4°C.
5) To wash the DNA pellet, the supernatant was discarded and 1 ml of 70% (vol/vol) ethanol at -20°C was added, vortexed briefly and centrifuged at 15 000 g for. This step was repeated once.
6) After the last wash most of the ethanol was removed from the samples and pellets was left to dry at RT and dissolved in 100 µl TE-buffer.

3.3.2 µChIP on NCCIT cells

In principal the procedure for small-scale ChIP is the same as for large scale ChiP so only the differences are pointed out here. Prior to this ChIP experiment, NCCIT cells were cultured, harvested, and cross-linked. The cross-linked cells were counted and diluted in order to get cell suspensions with 10 000 cells and 1000 cells for small-scale ChIP. The 10 000 or 1000 NCCIT cells were lysed by addition of 190 µl lysis buffer and sonicated for 3x30 or 4x30 seconds respectively. 400 µl RIPA buffer was added to the sonicated samples. The samples were mixed by vortexing and centrifuged at 12000 g for 10 min at 4°C. 550 µl of the supernatant was recovered into a new tube. 600 µl RIPA ChIP buffer was added to the remaining pellet, mixed

by vortexing and centrifuged as above. 550 µl of the supernatant was recovered and pooled with the first supernatant. Then 400 µl RIPA-ChIP buffer was added to the pooled chromatin to get a total volume of 1500 µl. The pooled diluted chromatin was suitable for 6 parallel ChIPs and 3 parallel input references. 150 µl of chromatin was used in each sample.

3.3.3 Fragmentation assessment

In order to obtain chromatin fragments of 400-500 bp, which has been proven to be suitable for ChIP-assay [66], the sonication conditions were tested. To test sonication conditions 8 samples with 100 000 NCCIT cells per sample were sonicated with increased time and the fragmentation size were visualized by agarose gel-electrophorese. Cross-linked and lysed NCCIT was divided into eight eppendorf tubes and sonicated for 1x30, 3x30, 6x30, 10x30, 14x30, 20x30 and 30x30 seconds. One tube was not sonicated. The DNA was purified using the phenol-chloroform-isoamylalcohol extraction methods as described and dissolved in 20 µl Milli-Q water and treated with RNAse (10mg/ml) on a thermoblock for 30 min at 37°C. To resolve DNA fragmentation size a 1,5% agarose solution was made by dissolving 1,5 gram of ultrapure agarose in 100 ml TBE buffer. Before casting in gel trays, 3 µl SYBR Safe DNA gel stain was added to the agarose solution. SYBR safe is a fluorescent dye that makes it possible to visualize DNA using a standard UV transilluminator. Samples were prepared by the addition of 6x loading dye and DNA. The agarose gel electrophoresis was run for 30 min at 150 volts, 400 mA, 100W in TBE running buffer. A DNA ladder containing DNA fragments of known sizes was run alongside the samples in the gel to provide a reference for DNA size.

3.3.4 ChIP on spermatogenic cells.

In general, ChIP assays on pachytene spermatocytes (PCS) and round spermatids (RS) were performed as for *ChIP on NCCIT cells (3.3.2)* and as described previously in the protocol *A rapid micro chromatin immunoprecipitation assay, Dahl et al. 2008* [66], with some modification.

3.3.5 Chromatin preparation

In brief fresh purified pachytene- and round spermatids cells resuspended in 1 ml PBS, were cross-linked with 27 µl formaldehyde and quenched by 114 µl glycine. Cross-linked cells were stored at -80°C. Cell lysis was performed by adding 200 µl lysis buffer to the cross-linked cells and vortexing as well as incubation for 5 min on ice. The chromatin of PCS and RS was sonicated for 18x30 or 24x30 respectively. The cell lysate was cleared by centrifugation (12,000g for 10 min at 4°C) and 180 µl of the supernatant was recovered. 13 µl of the supernatant was dedicated for fragmentation assessment. The DNA concentration was determined by A_{260} measurement and the sheared chromatin was either diluted to 0,13U in RIPA ChIP-buffer with 1% SDS, or diluted 10x in RIPA ChIP-buffer for storage at -80°C.

3.3.6 Test of different antibodies targeting the same epitope

Chromatin from PCS was tested with three different antibodies specific for H3K27me3, monoclonal and polyclonal antibody from Diagenode (cat#: mAb-181-050 and pAb-069-050) and a polyclonal antibody from Millipore (cat#:CS200603). Chromatin from RS was tested for two antibodies specific for H3K9me2, monoclonal and polyclonal antibody from Diagenode (cat#: mAb-154-050 and pAb-060-050)
In principle the procedure was the same as described for *ChIP on NCCIT cells (3.3.1)* so only the differences were pointed out. The chromatin preparation was carried out as above (*3.3.5 Chromatin preparation*). 120 µl of 0,13 U chromatin was used in each sample. The ChIP material was washed three times by 4-min incubations in 100 µl RIPA-buffer with 490 mM NaCl and 0,24% SDS. The ChIP samples were run in triplicates and duplicates for PCS and RS respectively.

3.3.7 Optimization of washing conditions for ChIP

0,13U chromatin from PCS and RS was used in ChIP experiments for test of stringency in the washing step. The procedure was the same as above (*3.3.6 Test of different antibodies targeting the same epitope*) except that the ChIP material was washed three times by 4-min incubations in either 100 µl RIPA-buffer with 140 mM NaCl and 0,1% SDS or 100 µl RIPA-buffer with 490 mM NaCl and 0,24% SDS.

3.3.8 Preparation of ChIP DNA from spermatogenic cells for ChIP-Seq

5 tubes with cross-linked PCS and 5 tubes with cross-linked RS from five independent spermatogenic cell purifications stored at -80 °C were used for ChIP to ChIP-seq. For the antibodies H3K4me3 (cat# pAb 003-050, Diagenode), H3k9me2 (cat# pAb 060-050 Diagenode) and H3K27me3 (cat# CS200603, Millipore), 6 µl was coupled to 30 µl Dynabeads Protein A in each ChIP sample, except TH2B (cat# 07-680, Upstate,Millipore) were 10 µl antibody was used. The cell lysis was performed by adding lysis buffer to each tube to a total volume of 200 µl and vortex as well as incubation for 5 min on ice. The chromatin of both cell types was sheared by 30 cycles sonication for 30 sec (Labsonic M, Ø 3 mm probe, cycle 0,5, 30% power, Sartorius). The cell lysate was cleared by centrifugation (11 700 g, 4°C for 10 min). About 150 µl of the supernatant from each tube was recovered and pooled into one tube for each cell type. 20 µl of the supernatant was dedicated for fragmentation assessment. The DNA concentration was determined by A_{260} measurement and the sheared chromatin was diluted to 0,2 A_{260}. Chromatin for ChIP with the antibodies H3K4me3, H3K27me3, and NoAb was diluted in RIPA buffer with 1% SDS. Chromatin for ChIP with the antibodies H3K9me2 and TH2B and the input samples were diluted in RIPA-buffer with 0,1%SDS. The diluted chromatin was applied to the respective primary antibody-bead complexes. 1,5 ml chromatin was transferred into each ChIP sample, except the input samples where 300 µl chromatin was added. The ChIP material was washed in RIPA with 0,24% SDS, except the ChIP with H3K9me2. DNA from precipitated chromatin and input samples were extracted by ethanol precipitation and dissolved in 15 µl EB-buffer. The EB-buffer was diluted 4x in MQ water.

3.4 Quantitative Real-time PCR (q-rtPCR)

Quantitative Real-time PCR (q-rtPCR) was used to quantify immunoprecipitated DNA from NCCIT cells, PCS cells and RS cells. It was also used to quantify c-DNA in gene expression analysis of PCS and RS. The quantitative PCR reactions were carried out on a Step One Plus Real-Time PCR system (Applied Biosystems) with Power SYBR green master mix and gene specific primers for selected target genes. The Power SYBR® Green PCR Master Mix contains SYBR® Green I Dye, AmpliTaq Gold® DNA Polymerase, UP, dNTPs, Passive reference and Optimized buffer components [74].

In real-time PCR, measurements are made in the exponential phase in contrast to traditionally PCR were results are collected after the reaction is completed (Fig. 7a). To monitor the accumulation of PCR products, the fluorescent reporter molecule SYBR® Green I Dye was used. The SYBR® Green I Dye binds to every double stranded DNA in the PCR reaction and fluorescence intensity is measured by the instrument. The increase in fluorescence intensity is proportional to the quantity of double stranded PCR product produced [75]. Two values are calculated by the instrument in the exponentially phase, the Threshold line and the Cycle Threshold. The Threshold line is the level of detection when the PCR reaction reaches a fluorescent intensity above background. The Cycle Threshold (Ct) is the PCR cycle when the sample reaches the threshold line (Fig. 7b). The amount of template DNA in an unknown reaction can be precisely determined by comparing the Ct value from the sample with unknown concentration with a dilution series of standard containing a range of known quantities (Fig. 7c) [76].

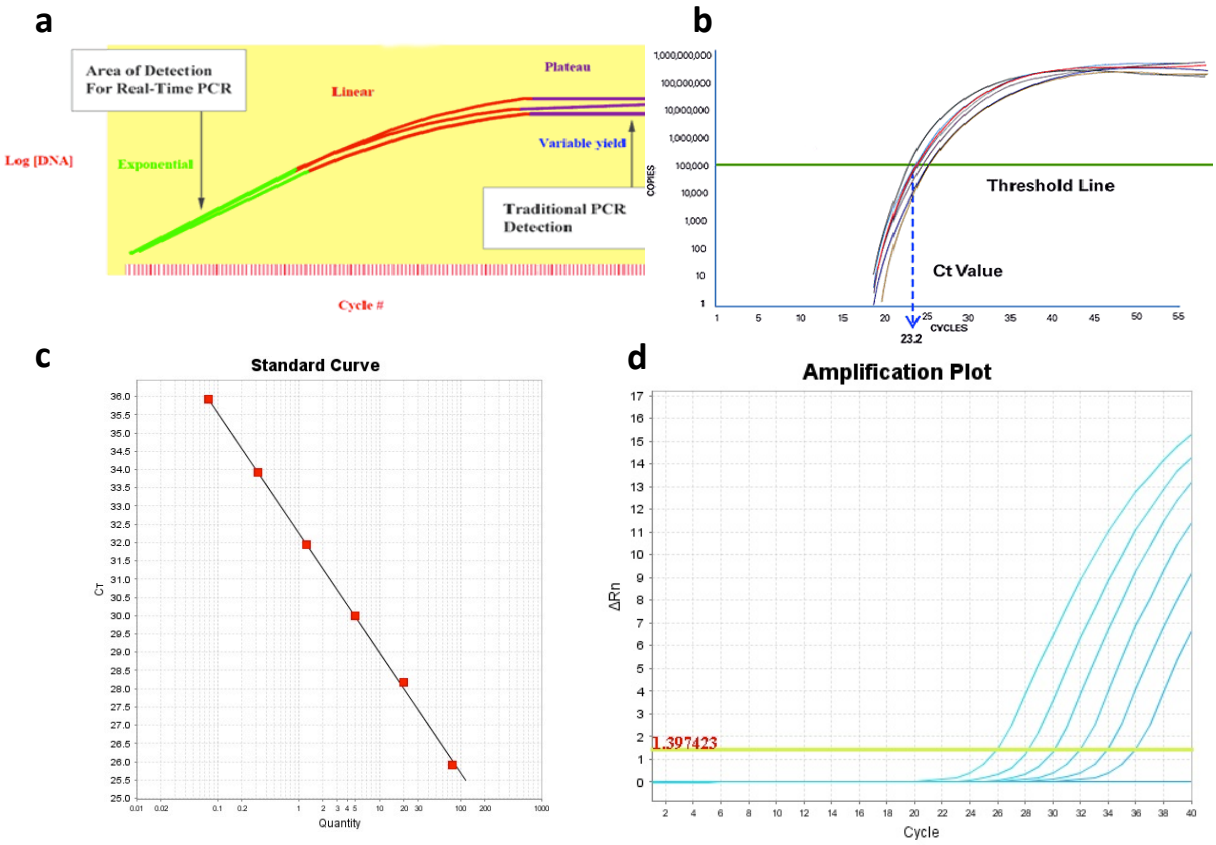

Figure 7: a) Area of detection for real-time PCR and endpoint PCR. **b)** The Cycle Threshold or Ct is the PCR cycle when the sample reaches a fluorescent intensity above background. **c)** Standard curve made of a dilution series of standards containing known quantities. **d)** Amplification plot of 5 samples. Figure a) and b) taken from *http://www.invitrogen.no* [76].

3.4.1 q-rtPCR on NCCIT cells

The quantification of chromatin immunoprecipitated DNA from NCCIT cells were performed on the Step One Plus Real-Time PCR system, with Power SYBR green master mix and gene specific primers for the target sequence human *Oct4pp*: forward 5'AGT CTG GGC AAC AAA GTG AGA 3' and reverse 5'AGA AAC TGA GGA GAA GGA TG 3'.

The concentration of DNA was determined by comparison to a standard curve made from a 4x dilutions series of DNA from NCCIT cells with a starting concentration of 20ng/µl. Seven standards were made. A non-template control was included to see primer dimers and contamination of the reaction. All samples were run in duplicates and with one technical parallel (2 runs per samples). To highlight the precipitation

efficiency and the extent of unspecific precipitation [66] the data was expressed as percent precipitated DNA relative to input.

Procedure:

1) A mastermix (Table 5) was prepared on ice in a 1,5 ml eppendorf tube for all samples to be quantified.
2) 16 µl of the mastermix and 4 µl of each samples and the standards were displaced in each well in the MicroAmpTM Fast Optical 96-Well Reaction Plate. 4 µl of MQ water was added to the well with the non-template control.
3) The reaction plate was mixed gently and centrifuged briefly and then loaded into Step One Plus Real-Time machine. PCR condition were 95°C for 5 min and 50 cycles of 95°C for 15 sec and 60°C for 1 min.

Table 5: q-rtPCR mastermix

Component	Volume (µl)	
	Per sample	Reaction mix X samples
Power SYBR® Green PCR Master Mix	10	X*10
Forward primer (20pmol/µl)	0,2	X*0,2
Reverse primer (20pmol/µl)	0,2	X*0,2
H2O	5,6	X*5,6
Total	16	X*16

3.4.2 q-rtPCR on PCS and RS cells

q-rtPCR on pachytene spermatocytes and round spermatids were carried out with the same conditions as for *q-rtPCR on NCCIT cells* (*3.4.1*). Primers for eight selected target genes were used (Table 6) and a mastermix for each target gene was made.

To quantify the precipitated DNA amount, fragmented DNA from germ cells from testes from C57/BL6 mice was used to make a standard curve. Germ cells were collected from one round of STA-PUT. Cells were cross-linked, sonicated 9x30 sec and DNA was purified using the phenol-chloroform-isoamylalcohol extraction method as described. The DNA concentration was measured on a Nanodrop ND-1000

Spectrophotometer (NanoDrop Technologies). It was made a 4x dilution series of DNA, with a starting concentration of 20 ng/µl. The DNA was diluted seven times.

Table 6: Primers used in q-rtPCR

Gene name	Forward primer	Reverse primer
Prm1	5' gcc ttg ggt tat cta tca 3'	5' tgt tca gtt agt cac tca 3'
Suv39h2	5' aac aga cag cac ctc tcc 3'	5' ttc act cca cac cac cag 3'
Hdac1	5' aag cct cgg cgt att ctc 3'	5' gcg tgt gca aag atc aga g3'
Meisetz	5' gag cag acc taa gca ctt 3'	5' gtg tta cct gac ctg tgt 3'
HoxD4	5' ctg ggt agg acc cga ggt tg 3'	5' ggc tgt aca att tca cca ggc 3'
Jhdm2a	5' ctt atc tgt gag cct gtg 3'	5' ttc ttc cat ttg ttg cct 3'
Nanog	5' cta tcg cct tga gcc gtt g 3'	5' aac tca gtg tct aga agg aaa gat ca 3'
Oct4	5' ctg taa gga cag gcc gag ag 3'	5' cag gag gcc ttc att ttc aa 3'

3.5 Reverse Transcription PCR

In order to quantify gene expression levels in pachytene spermatocytes and round spermatids, a Real-Time RT PCR experiment was conducted. Total RNA was extracted from snap frozen pellets of PCS and RS, and a reverse transcription PCR (RT-PCR) reaction synthesized cDNA from total RNA. The resulting cDNA was used as template in q-rtPCR.

3.5.1 Isolation of total RNA

RNAzol RT reagent was used to extract total RNA from snap frozen pellets of pachytene spermatocytes and round spermatids. The isolation was done according to the RNAzol protocol for isolation of total RNA with some adjustments [77]. Pellets were lysed and homogenized in RNAzol RT. Molecules like DNA, proteins and polysaccharides were precipitated from the lysate by adding diethylpyrocarbonate treated water (DEPC water), and removed by centrifugation. The RNA containing supernatant was precipitated by the addition of Polyacryl-carrier and isopropanol, followed by two washes in ethanol and solubilization in DEPC water.

Procedure:

1) Cell pellets of 100 000 – 300 000 cells were lysed and homogenized by adding 1 ml RNAzol, displacing the suspension to a tube containing Lysing Matrix D and then homogenized in a FastPrep instrument.
2) The homogenized cells were then transferred to a new 2 ml tube, 0,4 ml DEPC water was added and mixed for 15 seconds, stored at the bench for 15 min and then centrifuged at 12 000 g for 15 min.
3) One ml of the RNA containing supernatant was displaced to a new tube and RNA was precipitated by adding 2 µl Polyacryl-carrier and 1 ml of isopropanol, left 10 min on the bench and centrifuged at 12 000 g for 10 min.
4) The RNA pellet was washed twice by adding 0,5 ml 75% ethanol, mix and centrifuged 1 minute at 4000 g.
5) The supernatant was removed and the RNA pellet was dissolved, without drying, in 50 µl DEPC water.

3.5.2 DNase treatment of total RNA

To degrade any genomic DNA remnants from the RNA preparations, a TURBO DNA-free KIT was employed according to the manufactures protocol [78].

Procedure:

1) 5µl 10x TURBO DNase Buffer and 1 µl TURBO Dnase were added to 44 µl total RNA, mixed gently and incubated at 37^{o}C for 30 min.
2) After the incubation, 5µl of resuspended DNAse inactivation Reagent was added, mixed well and incubated at R.T for 2 min.
3) The suspension was centrifuged at 10 000 g for 1,5 min and the RNA supernatant was transferred to a fresh tube.

3.5.3 Quantification of RNA by photometric analysis

To determine concentrations and purity of RNA, a NanoDrop ND-1000 Spectrophotometer was used. Measurement at both 260 nm and 280 nm give an absorbance ratio $A_{260/280}$ and this ratio is used to assess the purity of RNA. For pure RNA the acceptable ratio is approximately 2,0. If the ratio is lower than the acceptable value, it may indicate presence of contaminants that absorb near 280 nm [79].

3.5.4 Reverse transcription of RNA to cDNA

A High Capacity cDNA Reverse Transcription Kit was used in order to synthesize single-stranded cDNA from total RNA. During the RT reaction random primers hybridizes to RNA and reverse transcriptase synthesizes a single-stranded DNA molecule complementary to the RNA. To determine genomic DNA contamination in the RNA samples, minus reverse transcriptase (-RT) controls were included. It is important that the RNA does not contain any genomic DNA because this may lead to false positive results in the q-rtPCR. A –RT control contains all the RT-PCR reagents except the reverse transcriptase. The reverse transcription reaction was carried out in duplicates, with an –RT control for each cell type. Equal amounts of total RNA (3 ng) from each cell type were used, and to avoid experimental variation they were processed simultaneously. The RNA concentrations were 3 ng. The High Capacity cDNA Reverse Transcription Kit was used according to manufactures protocol [80].

Procedure:

1) A 2X RT mastermix was prepared on ice in a 1,5 ml eppendorf tube for all total RNA samples to be reversed transcribed, mixed and spun down. A RT mastermix for – RT control was prepared in a separate tube (Table 7)
2) Six 0,2 ml PCR tubes were labelled, 4 for the samples and two for the –RT control.
3) 10 µl of the mastermix and 10 µl of each total RNA samples were displaced to the corresponding tube, mixed gently and centrifuged briefly.

4) The tubes were then loaded into a thermal cycler with conditions as follow: 25°C for 10 min, 37°C for 120 min and 85°C for 5 min.

Table 7: 2X RT mastermix

Component	Volume (µl)		-RT control
	Per sample	Reaction mix (x4)	Reaction mix (x2)
10X RT Buffer	2	8	4
25X dNTP Mix (100 mM)	0,8	3,2	1,6
10X RT Random Primers	2	8	4
MultiScribe Reverse Transcriptase	1	4	-
Nuclease-free H2O	3,2	12,8	8,4
Total	10	40	20

3.5.5 q-rtPCR on cDNA

q-rtPCR on cDNA was carried out with the same conditions as for *q-rtPCR on NCCIT cells* (*3.4.1*). Pre-designed primers *(table 8)* for seven selected target genes (*Jhdm2a*, *Nanog*, *HoxD4*, *Suv39h2*, *Prm1*, *Meisetz*, *Hdac1*) and two endogenous control genes (*Gapdh* and *β-Actin*) were used and a mastermix (Table 5) for each gene was made. A –RT control for each cell type was also included for each target gene to be amplified. The cDNA was quantified by comparison to a standard curve made from cDNA from the same stock of mixed cDNA from pachytene spermatocytes and round spermatids. It was made a 3x dilution series of the cDNA with a starting concentration of 1,25 ng/µl. As endogenous controls two housekeeping genes, glyceraldehyde 3-phosphate dehydrogenase (*Gapdh*) and *β-Actin* were used. The endogenous controls should be expressed at similar levels in all samples tested, and was used to normalize fluorescence signals for the target that are to be quantified.

Table 8: Primers used in q-rtPCR on cDNA

Gene name	**Forward primer**	**Reverse primer**
Nanog	5' caa gaa ctc tcc tcc att 3'	5' tga atc aga cca ttg cta 3'
HoxD4	5' tac cct tgg atg aag aag 3'	5' tgg tca gat acc tgt taa 3'
Hdac1	5' tgg tcg caa gaa ctc ttc 3'	5' ttc tgg ctt ctc ctc ctt 3'
Suv39h2	5' atg agt tca cag tgg atg 3'	5' gcc gag tat caa ggt tat 3'
Prm1	5' agc aaa agc agg agc aga 3'	5' cat cgc ctc ctc cgt ctg 3'
Meisetz	5' gaa gag aac taa gga cag aa 3'	5' agt gcg atg att cca ttc 3'
Jhdm2A	5' cgc cac atc agg ttc ata 3'	5' taa gcc aga agc agt gtt 3'

3.6 Qubit

In order to determine the concentration of ChiP DNA before whole genome sequencing, a Qubit® 2.0 Fluorometer together with Qubit™ dsDNA HS assay kit was used. The Qubit™ dsDNA HS assay kit contains Qubit™ dsDNA HS buffer, QubitTM dsDNA HS Standard #1, QubitTM dsDNA HS Standard #2 and QubitTM dsDNA HS Reagent (which is a fluorerscence-based dye that fluoresce when bound to DNA. The fluorescence are detected with a photodiode in the Qubit® 2.0 Fluorometer and the measurement was done according to the *Qubit® 2.0 Fluorometer, User Manual* [81].

Procedure:

1) A Qubit working solution was made for all samples and standards to be measured by diluting the Qubit™ dsDNA HS reagent 1:200 in Qubit™ dsDNA HS buffer.
2) 190 µl of QubitTM working solution was loaded into each of the tubes used for standards and 10 µl of each QubitTM standard was added to the appropriate tube and mixed by vortexing.
3) 199 µl of QubitTM working solution and 1 µl of samples was loaded into the corresponding tubes and vortexed.
4) All tubes were allowed to incubate at R.T. for 2 min.
5) Before measuring the samples, a calibration was done by measuring the two standards.

3.7 Whole-Genome Chromatin Immunoprecipitation Sequencing (ChIP-seq)

To globally map the location of the histone modifications H3K4me3, H3K9me2 and H3K27me3 in addition to the histone variant TH2B, High-throughput sequencing was performed on immunoprecipitated DNA from PCS and RS. The whole-genome ChIP sequencing was performed at Bejing Genomics Institute (BGI). For library-preparation the Illumina sample preparation kit was used and the sequencing was carried out using the Illumina/Solexa Genome Analyzer sequencing system. The experimental pipeline of ChIP-seq is showed in figure 8. ChIP DNA and Input samples were prepared for solexa sequencing by producing a DNA library of adapter modified fragments [82]. In brief the adapter modified fragments are made by DNA-end repair, 3'-dA overhang and ligation of sequencing adaptors. Adapter ligated DNA fragments are size fractionated in an agarose-gel and fragments of 200-500 bp are isolated via gel-extraction and amplified in a PCR reaction with limited cycles [83].

On the Illumina Cluster Station adapter-ligated ChIP DNA fragments are amplified on a solid flow cell substrate and clusters of clonal ChIP-DNA fragments are made. The clusters of clonal ChIP-DNA fragments on the flow cell surface are sequenced by Illumina Genome Analyzer.

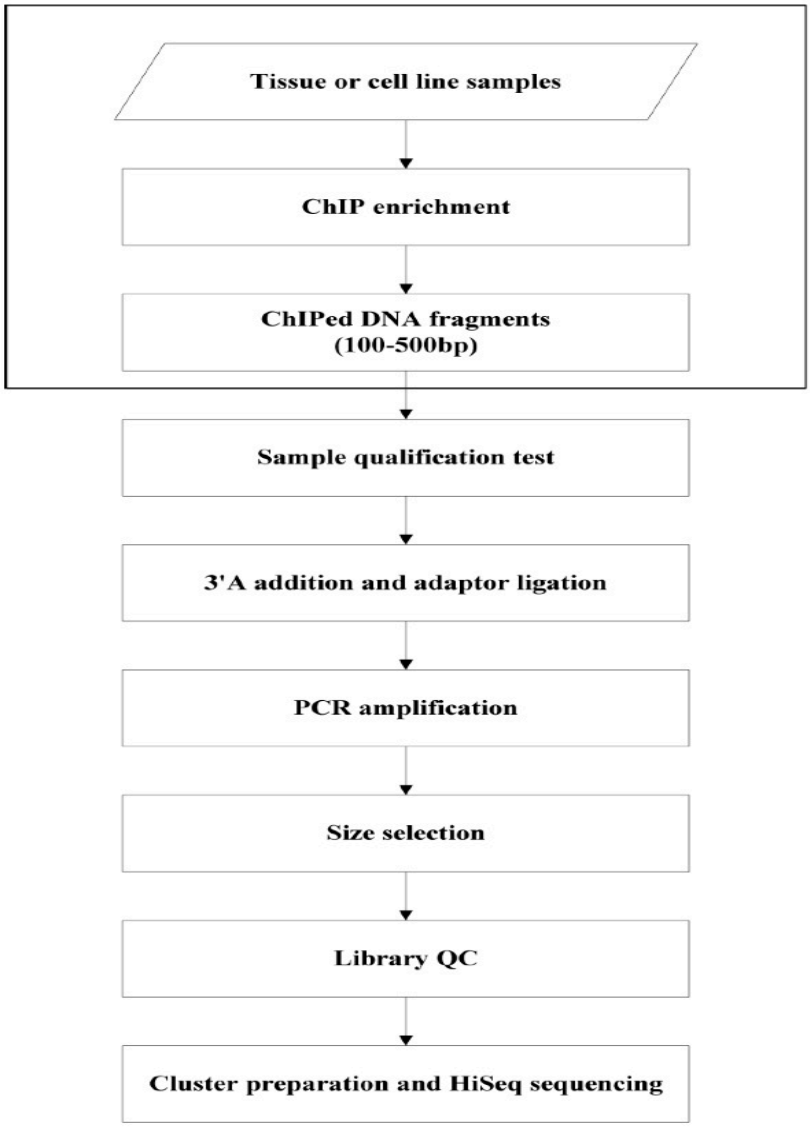

Figure 8: Experimental pipeline of ChIP-seq. Cell line samples were through ChIP enrichment. ChIP DNA was fragmented to 100-500bp by sonication. DNA-end was repaired to overhang a 3'-dA and adapters were ligated to the end DNA fragments. DNA fragments with proper size (200-300bp, including adaptor sequence) were selected after PCR amplification. Finally qualified library for sequencing was achieved. Figure taken from *BGI (BGI- www.genomics.cn)*

3.7.1 Mapping of sequenced reads and peak calling

For mapping (Fig. 9), the mm9 mouse genome was used as the reference genome. The July 2007 mouse (Mus musculus) genome data were obtained from the Build 37 assembly by NCBI and the Mouse Genome Sequencing Consortium. This assembly is also known as UCSC mm9. ChIP-Seq reads were mapped to the genome reference by SOAP. MACS version 1.4.0 was used with default parameters to identify regions of the genome significantly enriched in the histone modifications H3K4me3, H3K9me2, H3K27me3 and the histone variant TH2B.

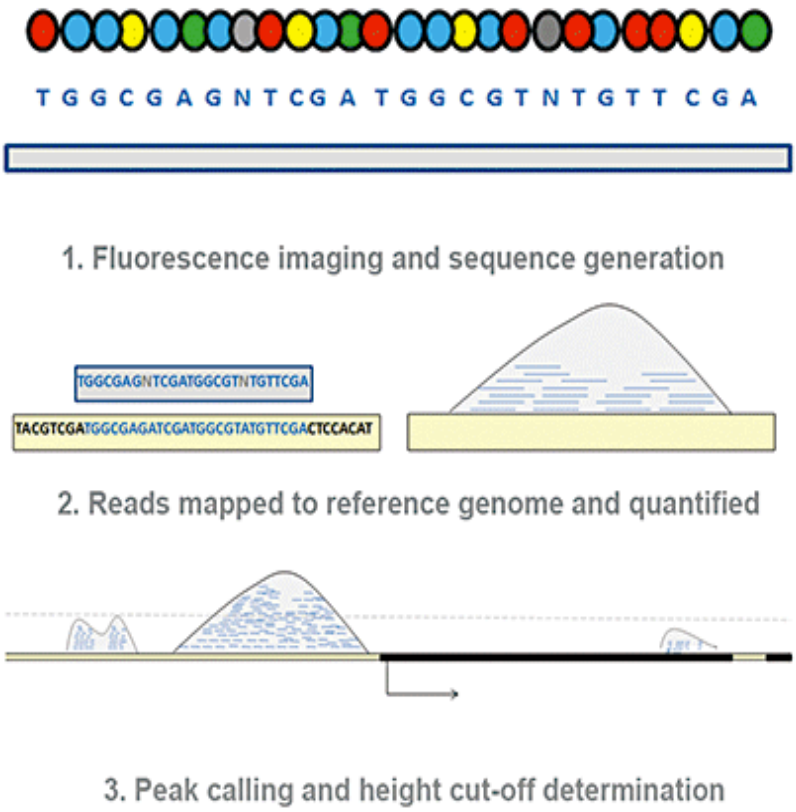

Figure 9: Mapping of sequenced reads and peak calling. 1) Colour images generated from Solexa sequencing are translated into nucleotide sequences, and **2)** mapped to a reference genome. **3)** The number of reads associated with genomic regions is analysed and regions of enrichment , or peaks are identified. Figure taken from *Cullum et al. 2011 [84].*

4 FRAMEWORK AND OBJECTIVES OF THE STUDY

Histone and histone variants have been shown to play an essential role in many cellular functions including DNA replication, DNA repair, mitosis, meiosis and regulation of gene expression. The role of histone modifications and variants in these cellular functions can be studied using the ChIP method. Such investigation can reveal the exact location of histone proteins and post-translationally modified histones in relation to gene regulatory regions or other genomic regions of functional relevance to the studied biology. Moreover, comparison of colocalization of various histone modifications or variants within and across cell types can shed light on the functional role of these histone modifications or variants.

My work has consisted in acquiring solid skills in several methods, with an emphasis on ChIP and STA-PUT and further applying those skills in the optimization of the ChIP conditions for PSC and RS in the assessment of three histone modifications and one histone variant. The established experimental conditions was first used for a pilot study of a panel of selected genes, and further laid the ground for ChIP-seq, resulting in genome-wide data which will be further analyzed after the completion of this thesis.

The objective of this study was to initiate the investigation of the role of the testis specific histone variant of H2B, i.e. TH2B, and the role of the developmentally important bivalent chromatin marks H3K27me3 and H3K4me3 in spermatogenesis. Several issues were addressed under these specific aims:

1) Assess experimental conditions of the ChIP procedure which could result in reduced background and an increased signal to noise ratio.
2) Identify the most promising commercially available antibodies for H3K27me3, H3K4me3, H3K9me2 and TH2B and determine experimentally which antibodies that perform best in distinguishing loci with high and low levels of the specific histone target.
3) Achieve isolation of PSC and RS at purity comparable to the best reported in the literature.
4) Achieve isolation of sufficient numbers of PCS and RS to allow for ChIP-seq.

5) Investigate the relationship, i.e. correlation in occupancy of TH2B with H3K9me2, H3K27me3 and H3K4me3 at the promoters of a selected number of genes to shed light on the role of TH2B.
6) Investigate the presence of bivalency of H3K4me3 and H3K27me3 at the same loci at promoter regions of selected genes in PCS and RS.
7) Achieve ChIP-seq data which can be used for further analysis of the relationships listed under point 5) and 6)

5 RESULTS

5.1 Initial optimization of the ChIP assay

Sonication of genomic DNA cross-linked to proteins is a crucial step in all ChIP projects. Sonication conditions were initially tested for 8 samples with 100 000 NCCIT cells per sample with increasing sonication time. The fragmentation size was visualized by agarose gel-electrophoreses. As expected, increased sonication time resulted in smaller DNA fragments (Fig. 10).

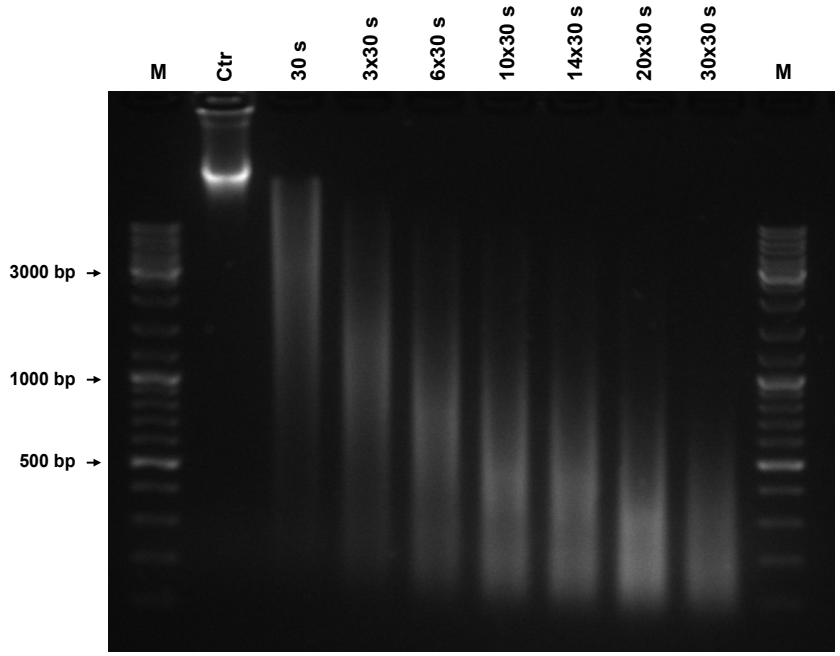

Figure 10: Agarose gel electrophoresis assessment of chromatin after increased sonication regimes. *M: Gene ruler DNA ladder mix*.

ChIP was initially optimized with chromatin from 100 000 and 10 000 NCCIT cells with H3K4me3 antibody. The level of this histone modification at the promoter of *Oct4* was assessed by q-rtPCR. The q-rtPCR data revealed higher precipitation efficiency and increased standard deviation between replicates with 10 000 cells (Fig. 11). In order to reduce NoAb background of unspecifically bound chromatin, we modified the ChIP procedure; the ChIP samples were subjected to vortexing when adding fresh washing solution, rather than gentle agitation. This physically rough

treatment of ChIP samples lead to comparable background levels despite of a reduction in cell numbers from 100 000 to 10 000 cells.

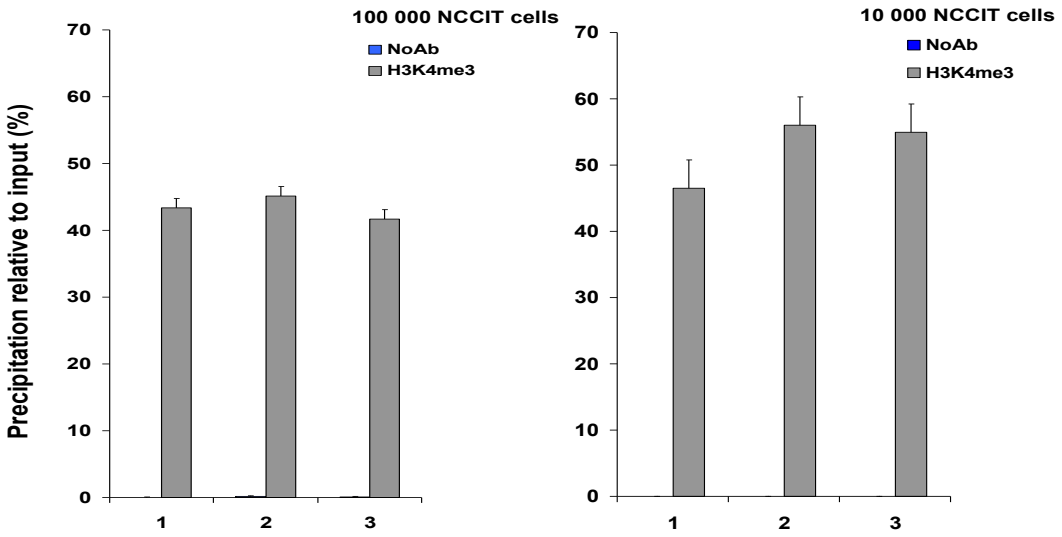

Figure 11: ChIP on NCCIT cells. ChIP was performed with chromatin from 100 000 and 10 000 NCCIT cells. The enrichment of H3K4me3 on the promoter of *Oct4* was assessed. The high and low cell number ChIP experiments were both performed in triplicate, and assessed by duplicate q-rtPCR for each replicate.

5.2 Isolation and validation of PCS and RS

Cells from two different spermatogenic cell stages, pachytene spermatocytes and round spermatids, were isolated from C57/BL6 wild type mice testes using the STA-PUT technique (Fig. 12). Testes from six mice were used in each round of STA-PUT, and the amount of PCS cells and RS cell isolated each round were on average $1{,}6x10^6$ and $> 4{,}0\ x10^6$, respectively.

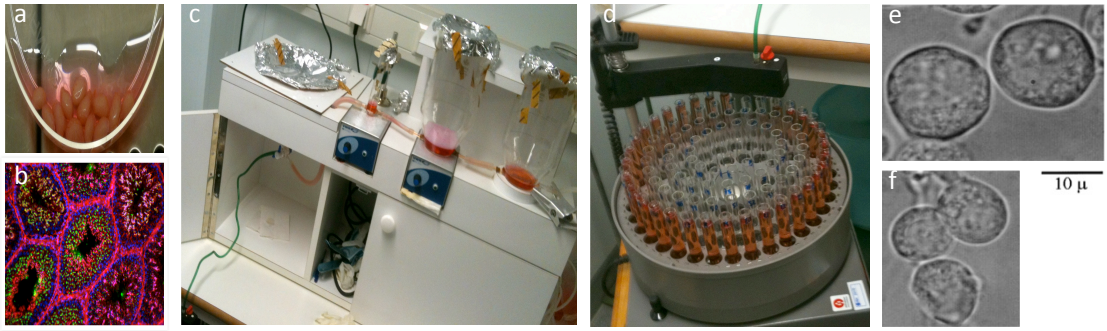

Figure 12: Isolation of PCS and RS. a) Testis from six C57/BL6 mice. **b)** Multicolor fluorescence image of mouse testis, cross-section**. c)** The STA-PUT apparatus. **d)** Automatic fraction collector. **e) f)** Phase contrast micrographs of PCS and RS respectively. Picture b taken from *http://www.invitrogen.com/site/us/en/home/support/Research-Tools/Image-Gallery/Image-Detail.2187.html.* Picture e and f modified from *Santi C M et al. J Gen Physiol 1998;112:33-53*

To assess the purity of the pachytene spermatocytes and round spermatids, cells were stained with fluorescent dyes using antibodies against proteins unique for these cells (Fig 13). The pachytene spermatocyte cells were stained with the primary antibodies anti-phospho-Histone H2AX and anti-SCP3 (Synaptonemal Complex 3). Phosphorylated H2AX (γ-H2AX) localizes to the XY body in the pachytene stage of spermatogenesis. The SCYP3 protein is a component of the synaptonemal complex formed during prophase 1 of meiosis, between homologous chromosomes. Round spermatids were stained with Lectin PNA that is specific for acrosome. In addition both cell types were counterstained with DAPI that stained the DNA blue. The stained cells were examined under an Axio Observer. Z1 plan 2 microscope and hundred PCS or RS cells were examined on each slide made from each round of purification. The pachytene spermatocytes were found to have a purity of 83% and the round spermatids showed a purity of 82%.

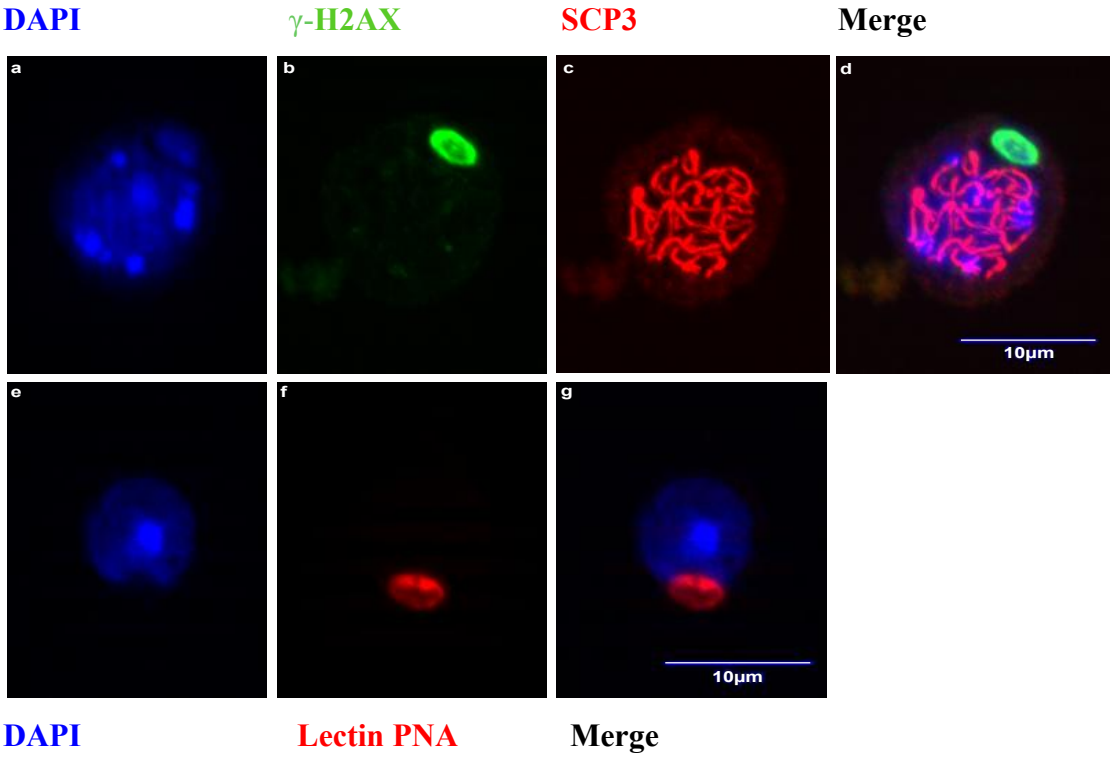

Figure 13: Immunofluorescence staining of pachytene spermatocytes and round spermatids. Pachytene spermatocytes were stained with **a)** DAPI, **b)** γ-H2AX , **c)** SCP3, **d)** merging of picture a, b and c. Round spermatids were stained with **e)** DAPI, **f)** Lectin PNA and **g)** merging of picture e and f.

PCS and RS isolated from five independent spermatogenic cell purifications (STA-PUT) were used for ChIP to ChIP-seq. The purity of the PCS and RS was on average 83% and 82%, respectively (Table 9). The average cell size was 11,5 µm for PCS and 8,5 µm for RS.

Table 9: Purity of PCS and RS. PCS and RS isolated from five independent spermatogenic cell purifications (STA-PUT) were used for ChIP to ChIP-seq. **a)** Purity of pachytene spermatocytes. **b)** Purity of round spermatids

a)

Pachytene spermatocytes			
ID	Number	Size (µm)	Purity (%)
1	$1,4x10^6$	12,1	-
2	$1,6x10^6$	11,1	85
3	$1,5x10^6$	11,5	86
4	$1,1x10^6$	11,1	80
5	$2,3x10^6$	11,7	80
Total/average	$7,9x10^6$	11,5	83

b)

Round spermatides			
ID	Number	Size (µm)	Purity (%)
1	$< 1,0x10^7$	8,4	80
2	$< 1,0x10^7$	8,9	87
3	$7,2x10^6$	8,5	83
4	$5,0x10^6$	8,4	81
5	$3,2x10^6$	8,5	78
Total/average	$< 1,0x10^7$	8,5	82

5.3 Optimization of washing conditions for ChIP

120 µl 0,13U chromatin from PCS and RS was used in a ChIP experiment with antibodies against H3K4me3, H3K9me2, H3K27me3 and TH2B for test of stringency in the washing step. The ChIP material was washed three times by 4-min incubations in either 100 µl RIPA-buffer with 140 mM NaCl and 0,1% SDS (from now on called RIPA-buffer with 0,1% SDS) or 100 µl RIPA-buffer with 490 mM NaCl and 0,24% SDS (from now on called RIPA-buffer with 0,24% SDS). Quantitative PCR (qPCR) was performed on loci known to have high and low levels of the histone modifications and variant to validate the outcome of increased stringency. ChIP samples with antibody against H3K4me3 (Fig. 14a and b) showed a slightly higher precipitation efficiency when washed in 0,1% RIPA-buffer. The H3K9me2 samples (Fig. 14 d and e) showed a decrease in precipitation efficiency when washed in RIPA-buffer with 0,24 % SDS. The H3K27me3 antibody (Fig. 14g) was tested directly in ChIPs with high stringency RIPA buffer (RIPA buffer with 0,24% SDS) and showed an enrichment of almost 150 between the high and low target gene for this histone modification (Fig. 14h). The TH2B antibody (Fig. 14i-j) showed a precipitation efficiency of 4% on the *Nanog* promoter and 1,4% on the *Jhdm2a* promoter with the 0,1% SDS RIPA-buffer. In washes with RIPA-buffer with 0,24% SDS the precipitation efficiency was 2,8% and 0,4% for *Nanog* and *Jhdm2a* respectively, thus the wash in 0,24% RIPA-buffer gave a higher fold enrichment (Fig. 14k) than the wash in 0,1% buffer for TH2B.

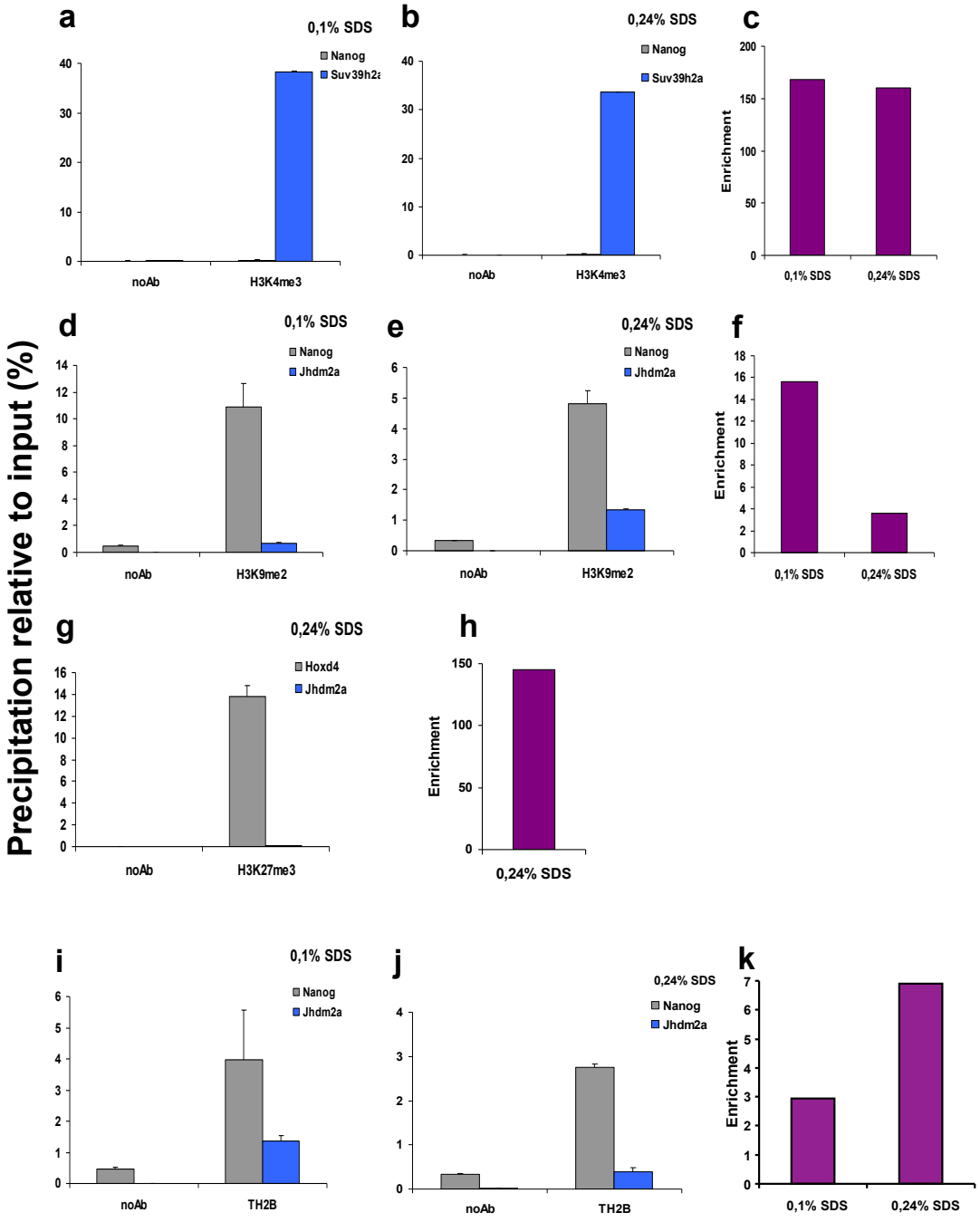

Figure 14: Optimization of ChIP washing conditions. Washes in RIPA-buffer with 140 mM NaCl and 0,1% SDS (called 0,1% SDS) and RIPA-buffer with 490 mM NaCl and 0,24% SDS (called 0,24% SDS) was tested for each antibody. The precipitation efficiency was visualized in q-rtPCR for selected target genes known to have high and low enrichment for the respective antibody. Enrichment reflects the ratio of our selected genes with the highest level of the relevant histone modification over that of our genes with the lowest level of the same modification.

5.4 Comparison of different antibodies targeting the same epitope and the effect on ChIP efficency

Chromatin from PCS was tested with three different antibodies specific for H3K27me3, monoclonal and polyclonal antibody from Diagenode (cat# mAb-181-050 and pAb-069-050) and a polyclonal antibody from Millipore (cat# CS200603). Chromatin from RS was tested for two antibodies specific for H3K9me2, monoclonal and polyclonal antibody from Diagenode (cat# mAb-154-050 and pAb-060-050)
120 µl of 0,13 U chromatin was used in each sample. To evaluate the precipitation efficiency for the aforementioned antibodies, each ChIP-sample was analyzed with primers for loci we know have high and low enrichment for each histone modification in real-time PCR. Loci with high and low enrichment of H3K9me2 and H3K27 have previously been identified (unpublished data). The monoclonal Ab against H3K9me2 had a precipitation efficiency of around 2% whereas the polyclonal Ab showed an efficiency of around 11% for the Nanog promoter (Fig. 15a). For the *Jhdm2a* loci, the mono- and polyclonal H3K9me2 antibody obtained a precipitation efficiency of 0,2 % and 2,1% respectively (Fig. 15b). In relation to the enrichment obtained by these antibodies, monoclonal H3K9me2 had a higher fold enrichment compared to the polyclonal H3K9me2 (Fig. 15c). In relation to the histone modification H3K27me3 (Fig. 15d and e), the polyclonal H3K27me3 from Diagenode showed the highest precipitation efficiency for both HoxD4 and *Jhdm2a* loci. The monoclonal antibody from Diagenode displayed the lowest efficiency, while the polyclonal Ab from Millipore presented highest fold enrichment (Fig. 15f).

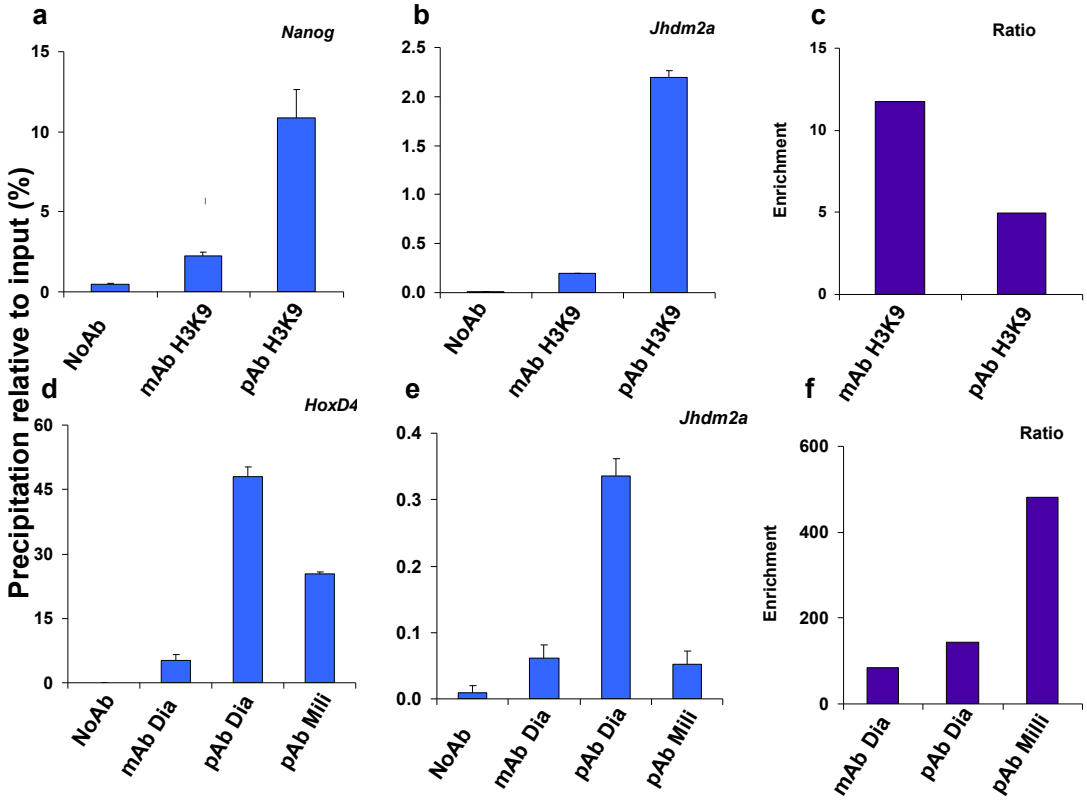

Figure 15: Comparison of different antibodies targeting the same epitope and the effect on ChIP efficiency. The ChIP experiments were performed in either duplicate or triplicate for all antibodies, and assessed by duplicate q-rtPCR for each replicate. **a), b)** The graphs shows the analysis of monoclonal and polyclonal H3K9me2 from Diagenode and no-antibody (NoAb) as a negative control, binding to the *Nanog* (a) and *Jhdm2a* (b) promoters. **c)** The graph shows the ratio of enrichment of mono- and poly-clonal H3K9me2 **d), e)** The graphs shows the analysis of mono- and polyclonal H3K27me3 from Diagenode, polyclonal H3K27me3 from Millipore and NoAb binding to the *HoxD4* (d) and *Jhdm2a* (e) promoters. **f)** The graph shows the ratio of enrichment of mono- and polyclonal H3K27me3 from Diagenode and polyclonal H3K27me3 from Millipore In figure a),b),d) and e) data are expressed as percent precipitation relative to input chromatin (mean values ± s.d). Enrichment c) and f) reflects the ratio of our selected genes with the highest level of the relevant histone modification over that of our genes with the lowest level of the same modification *mAb Dia*: monoclonal antibody from Diagenode; *pAb Dia*: polyclonal antibody from Diagenode; *pAb Milli*: polyclonal antibody from Millipore.

5.5 Occupancy of the histone variant TH2B and the histone modifications H3K4me3, H3K9me2 and H3K27me3 on gene promoters

0,13U chromatin from PCS and RS was used in ChIP experiments with antibodies against H3K4me3, H3K9me2, H3K27me3 and TH2B to assess histone modifications profiles at proximal promoters (PP) of the transcription factors genes *Nanog*, *HoxD4* and *Oct4*; the histone methyltransferases *Suv39h2* and *Meisetz*; the histone demethylase *Jhdm2a*; the histone deacetylase *Hdac1* and the protamine gene *Prm1*.

Note that the immunoprecipitation efficiency is antibody dependent. Therefore the level of precipitation cannot be directly compared between antibodies.

The testis specific histone variant TH2B (Fig. 16a) showed relatively high enrichment at the *Nanog*, *HoxD4* and *Oct4* promoters. The promoters of *Suv39h2, Meisetz* and *Prm1* also showed a relatively high enrichment of TH2B, while there were lower levels of TH2B on *Jhdm2a* and *Hdac1* promoters.

The histone modification H3K9me2 (Fig. 16b) correlated well with the TH2B profile on all gene promoters tested.

H3K27me3 (Fig. 16c) showed high levels at the *Hoxd4* promoter, with a decline to about the half from the pachytene to the round spermatid stage. We found an intermediate level of H3K27me3 on *Oct4. Prm1* showed a slight enrichment of H3K27me3 in PCS while there where hardly any occupancy of this histone modification at this site in RS. *Suv39h2*, *Meisetz*, *Jhdm2a* and *Hdac1* showed very low levels of H3K27me3 for both cell types. In summary the level of H3K27 was high at the genes with the highest H3K9me2 and TH2B levels i.e. the *Hoxd4* and *Oct4* promoter.

The level of the histone modification H3K4me3 (Fig. 16d) were high at promoters of the methyltransferases *Suv39h2* and *Meisetz*, the demethylase *Jhdm2*a and the deacetylase *Hdac1* at both cell stages. The *HoxD4*, *Oct4* and *Prm1* locus showed lower levels of H3K4me3 compared to the aforementioned gene promoters. With the exception of the *Suv39h2* promoter, there was an increase in the H3K4me3 level from the PCS to the RS stage for the rest of the genes harboring high levels of this mark: *Meisetz, Jhdm2a* and *Hdac1*

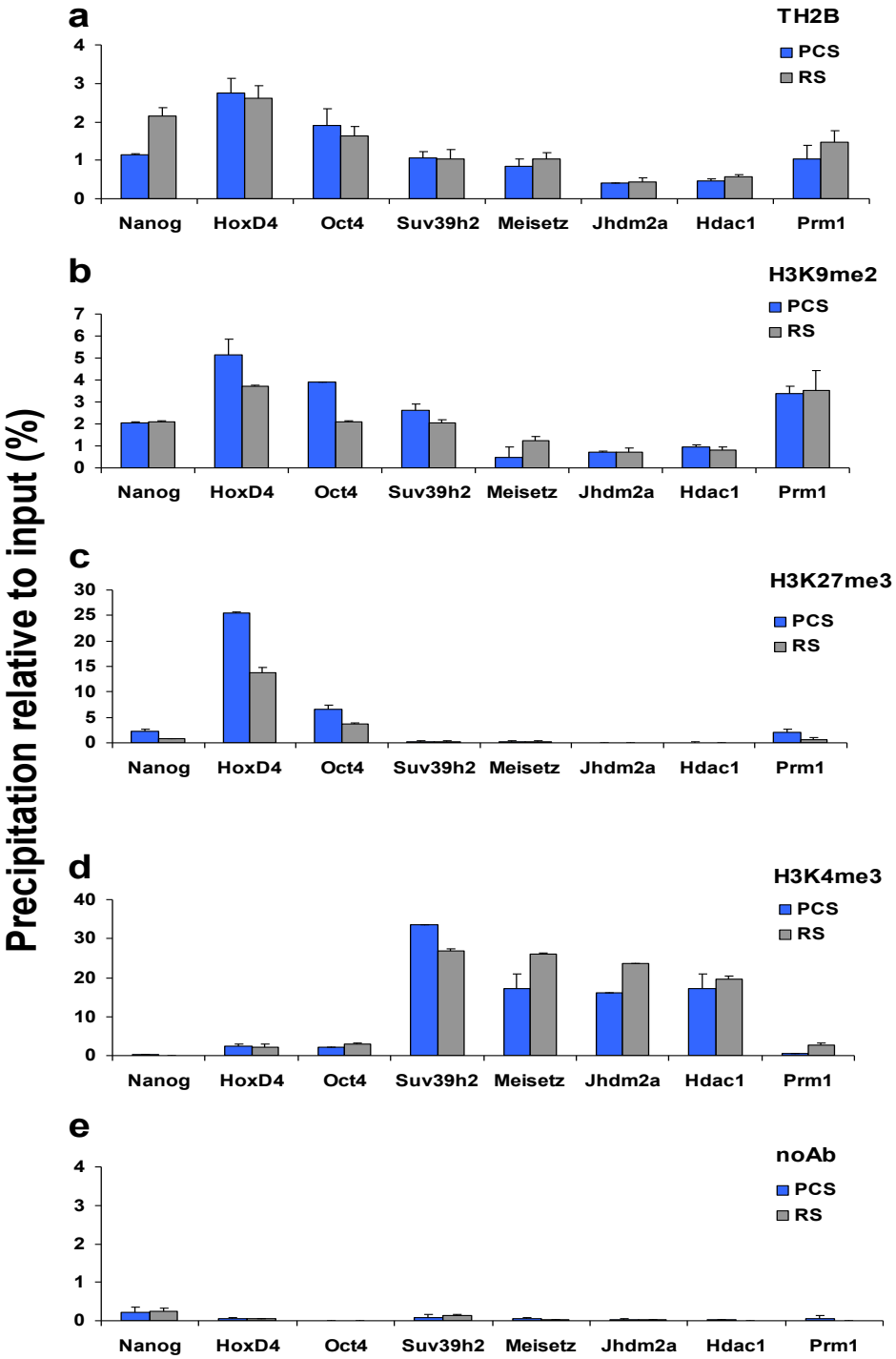

Figure 16: Occupancy of the histone modifications H3K4me3, H3K9me2, H3K27me3 and the histone variant TH2B at gene regulatory regions in PCS and RS. Levels of TH2B, H3K9me2, H3K27me3 and H3K4me3, were assessed by ChIP and subsequent q-rtPCR for the promoters of the pluripotency genes *Nanog, HoxD4* and *Oct4*; the histone methyltransferases *Suv39h2* and *Meisetz*; the histone demethylase *Jhdm2a*; the histone deacetylase *Hdac1*; and the protamine 1, *Prm1*. Data is presented as precipitation relative to input. **a)** TH2B enrichment, **b)** H3K9me2 enrichment, **c)** H3K27me3 enrichment, **d)** H3K4me3 enrichment and **e)** enrichment of NoAb as a control of the background unspecific precipitation.

5.6 Correlation analysis between TH2B and H3K4me3, H3K9me2 and H3K27me3

To test whether the histone modifications H3K4me3, H3K9me2, H3K27me3 and the histone variant TH2B correlate with each other at the proximal promoters of *Nanog*, *HoxD4*, *Oct4*, *Suv39h2*, *Meisetz, Jhdm2a*, *Hdac1* and *Prm1* the Pearson correlation coefficient was calculated (R^2). The histone variant TH2B showed a negative correlation with the histone modification H3K4me3 (Fig. 17a). H3K9me2 and H3K27me3 are described as repressive histone modifications in the literature [15] and there was a strong linear correlation between TH2B and H3K9me2 (Fig. 17b). The same trend was seen between TH2B and H3K27me3 (Fig. 17c). In both the two aforementioned cases there was a stronger positive correlation between RS than PCS. H3K4me3 showed a negative correlation with both the repressive marks H3K9me2 and H3K27me3 (Fig. 17d and e). The correlation between the repressive marks H3K9me2 and H3K27me3 was positive. In summary, TH2B associated strongly and significantly correlates with the repressive marks H3K9me2 and H3K27me3 at the tested gene promoters.

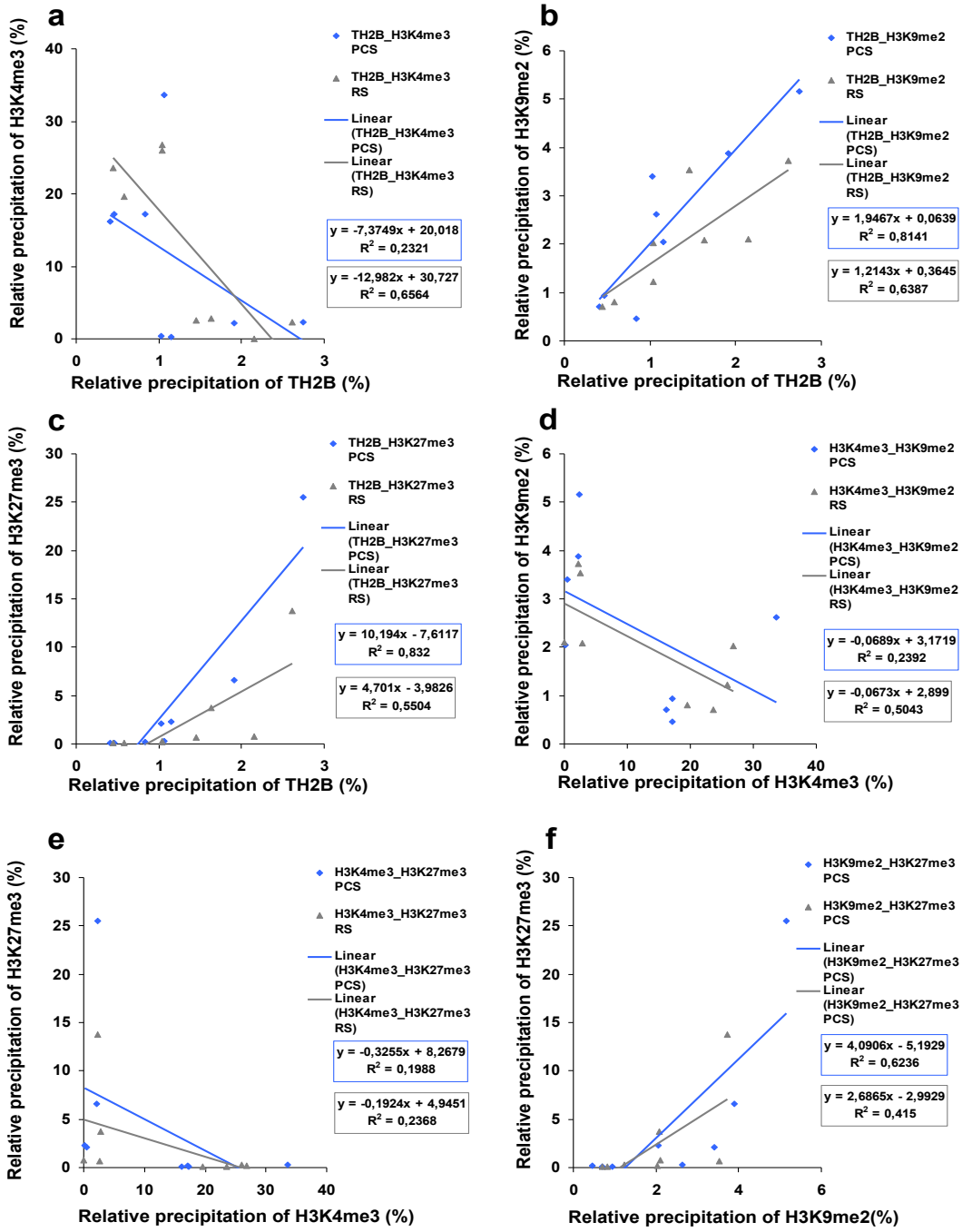

Figure 17: Correlation analysis of H3K4me3, H3K9me2, H3K27me3 and TH2B. To analyze whether the levels of H3K4me3, H3K9me2, H3K27me3 and TH2B correlate with each other at the proximal promoters of *Nanog, HoxD4, Oct4, Suv39h2, Meisetz, Jhdm2a, Hdac1* and *Prm1* the Pearson correlation coefficient was calculated (R^2). In detail linear correlation was tested between **a)** TH2B and H3K4me3, **b)** TH2B and H3K9me2, **c)** TH2B and H3K27me3, **d)** H3K4me3 and H3K9me2, **e)** H3K4me3 and H3K27me3 and **f)** H3K9me2 and H3K27me3. To conclude whether it is a negative or positive association (negative or positive slope) the linear equations were plotted as well.

5.7 Gene expression analysis of a pilot test panel of genes in PCS and RS

To explore the link between analyzed histone modifications and variant with expression of the respective genes, we synthesized cDNA from PSC and RS and determined the mRNA levels for *Suv39h2*, *Meisetz*, *Jhdm2a*, *Hdac1*, *Prm1* and the housekeeping genes *Gapdh* and *Actb* by real-time PCR. Table 10 shows cycle threshold (C_t) values from the real-time PCR experiment.

The chromatin modifying enzymes *Suv39h2, Meisetz, Jhdm2a* and *Hdac1* all showed significant levels of expression in both PCS and RS (Fig. 18b and table 10) and they all had enrichment of the histone modification H3K4me3 on their promoters (Fig. 16d).

The HMTase Suv39h2 and *Meisetz* showed increased expression upon meiotic progression (Fig. 18b) and the level of H3K4me3 followed this trend at the promoter of *Meisetz* but not on the *Suv39h2* promoter (Fig. 16d). The level of the facultative repressive mark H3K9me2 (Fig. 16b) correlated with the change in expression of *Suv39h2*, as the level of H3K9me2 decreased from the PCS to the RS stage at this promoter (Fig 18b). The demethylase *Jhdm2a* and the deacetylase *Hdac1* showed decreased expression upon meiotic progress (Fig. 18b), while the enrichment of H3K4me3 increased upon progression (Fig 16d). The *Prm1* gene showed relatively high expression, while the enrichment of H3K4me3 at this locus was low. The assessed repressive histone modification as well as TH2B showed quite high levels at the *Prm1* gene

Table 10 : C_t values from q-rtPCR where cDNA isolated from PCS and RS was used as template.

Gene	*Actb*	*Gapdh*	*Suv39h2*	*Meisetz*	*Jhdm2a*	*Hdac1*	*Prm1*
PCS	24	28	32	35	27	23	25
RS	24	28	29	32	28	24	22

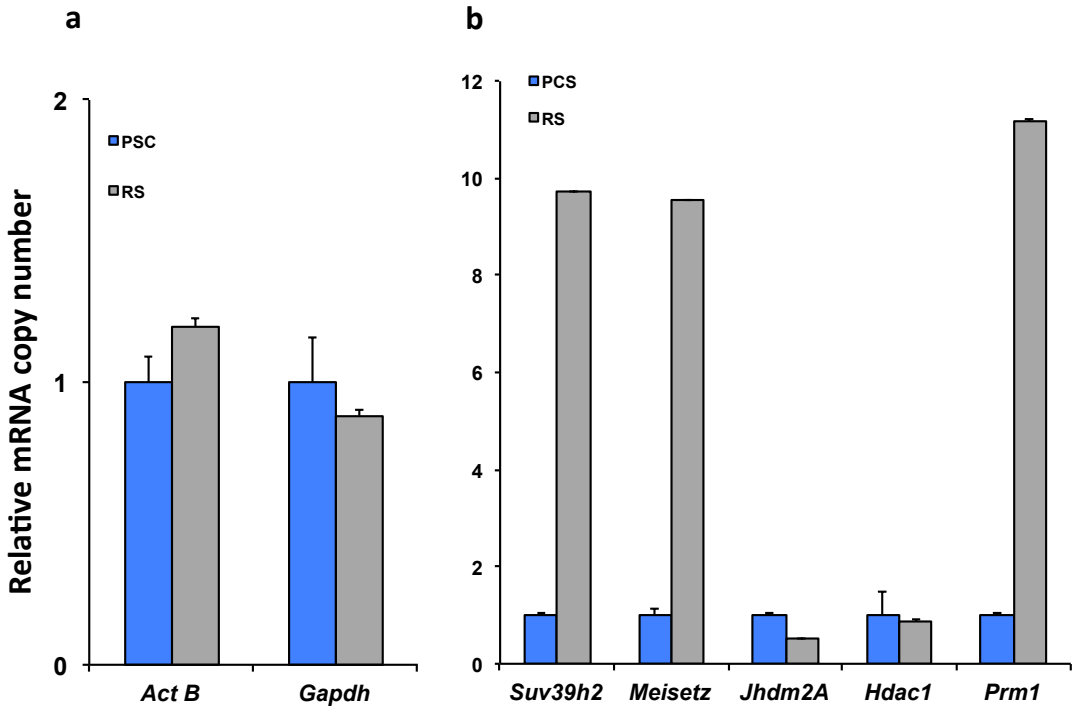

Figure 18: mRNA expression in spermatogenic cells. Quantitative reverse transcription polymerase chain reaction of *ActB, Gapdh*, *Suv39h2, Meisetz, Jhdm2a, Hdac1, and Prm1* **a)** The expression of *ActB* and *Gapdh*, normalized to the expression in PCS (PCS set to 1). **b)** The expression of *Suv39h2, Meisetz, Jhdm2a, Hdac1, and Prm1* relative to the expression of *Gapdh* normalized to the expression in PCS (mean ± s.d from three replicates in q-rtPCR).

5.8 Preparation of Chip DNA from spermatogenic cells for ChIP-Seq

We wanted to investigate the genome-wide distribution of the histone modifications H3K4me3, H3K9me2, H3K27me3 and the histone variant TH2B in pachytene spermatocytes and round spermatids. In this context we performed ChIP, and sent our ChIP-DNA samples to Bejing Genomics Institute (BGI) for whole genome sequencing. PCS and RS isolated from five independent spermatogenic cell purifications (STA-PUT) were used for ChIP to ChIP-seq. The purity of the PCS and RS was on average 83% and 82%, respectively. The cell size was on average 11,5 µm for PCS and and 8,5 µm for RS. The chromatin of both cell types was sheared by 30 cycles sonication for 30 sec and gave chromatin fragments with a major size of 200-600bp (Fig. 19). The ChIP was performed with the antibodies H3K4me3, H3k9me2, H3K27me3 and TH2B. 1,5 ml or 300 µl chromatin with the concentration 0,2 A_{260} where used in the ChIP-samples and input samples respectively. Before sending the

ChIP samples to BGI the concentration of chromatin were measured on a Qubit® 2.0 Fluorometer (Fig. 20). To perform whole-genome sequencing it was required a DNA quantity above 10 ng, and all samples showed concentration above this limit.

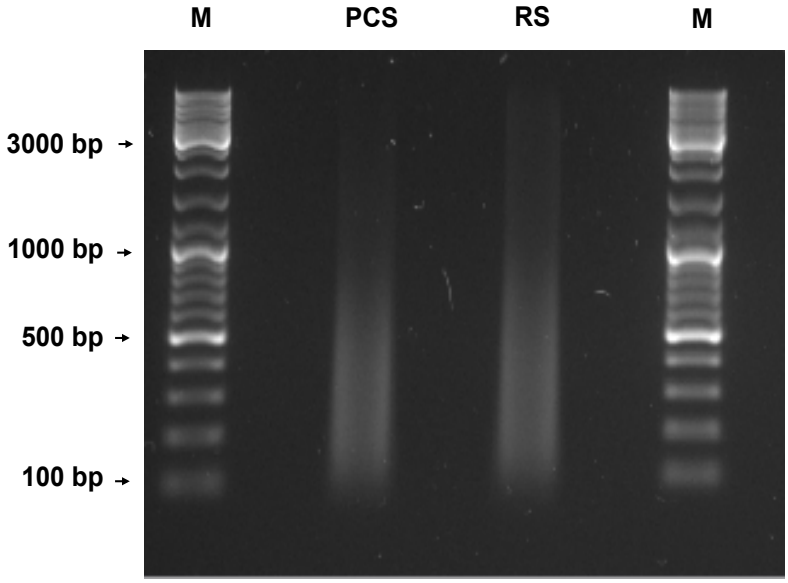

Figure 19: Fragmentation assessment of chromatin. ChIP chromatin from pachytene spermatocytes (PCS) and round spermatids (RS) was sheared by sonication 30 cycles for 30 s, yielding fragments with the sizes of 200-600 bp. M: *Gene ruler DNA ladder mix.*

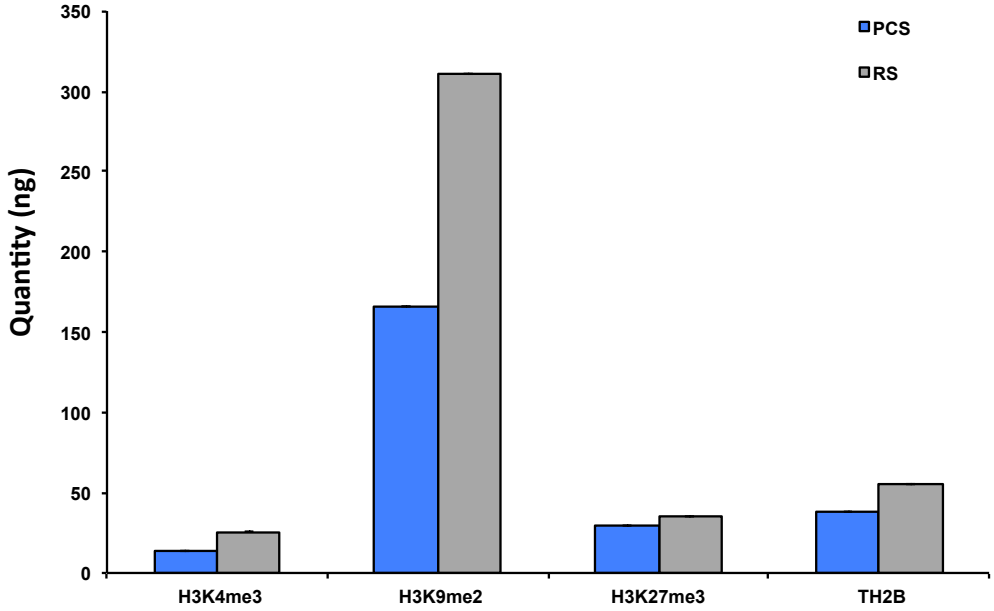

Figure 20: Total precipitated ChIP DNA. The quantity (ng) of ChIP DNA from PCS and RS was measured on a Qubit® 2.0 Fluorometer.

For optimum sequencing results, high quality of DNA is essential; therefore ChIP samples were checked for their quality by q-rtPCR prior to whole-genome sequencing. Each ChIP-sample was analyzed with primers for loci we know have high and low enrichment for each histone modification and histone variant (unpublished data). As expected, the H3K4me3 modification showed high enrichment on the *Suv39h2* promoter for both PCS and RS and almost no enrichment on the *Nanog* promoter (Fig. 21a). The precipitation efficiency of H3K9me2 was 8% for PCS on the *Nanog* promoter (Fig. 21b). Due to a technical error, likely because template was not distributed to the relevant PCR plate wells, there was not obtained any results for the RS sample on this gene. At the *Jhdm2a* loci PCS and RS showed a precipitation efficiency of 0,5% and 1,4% respectively (Fig. 21b). The histone modification H3K27me3 showed a precipitation efficiency above 20% for both PCS and RS on the *Hoxd4* loci and below 0,4% on the *Jhdm2a* loci (Fig. 21c) The *Nanog* promoter showed an enrichment of TH2B of above 2% for both PCS and RS. The enrichment for this histone variant was below 0,6% for both PCS and RS (Fig 21d).

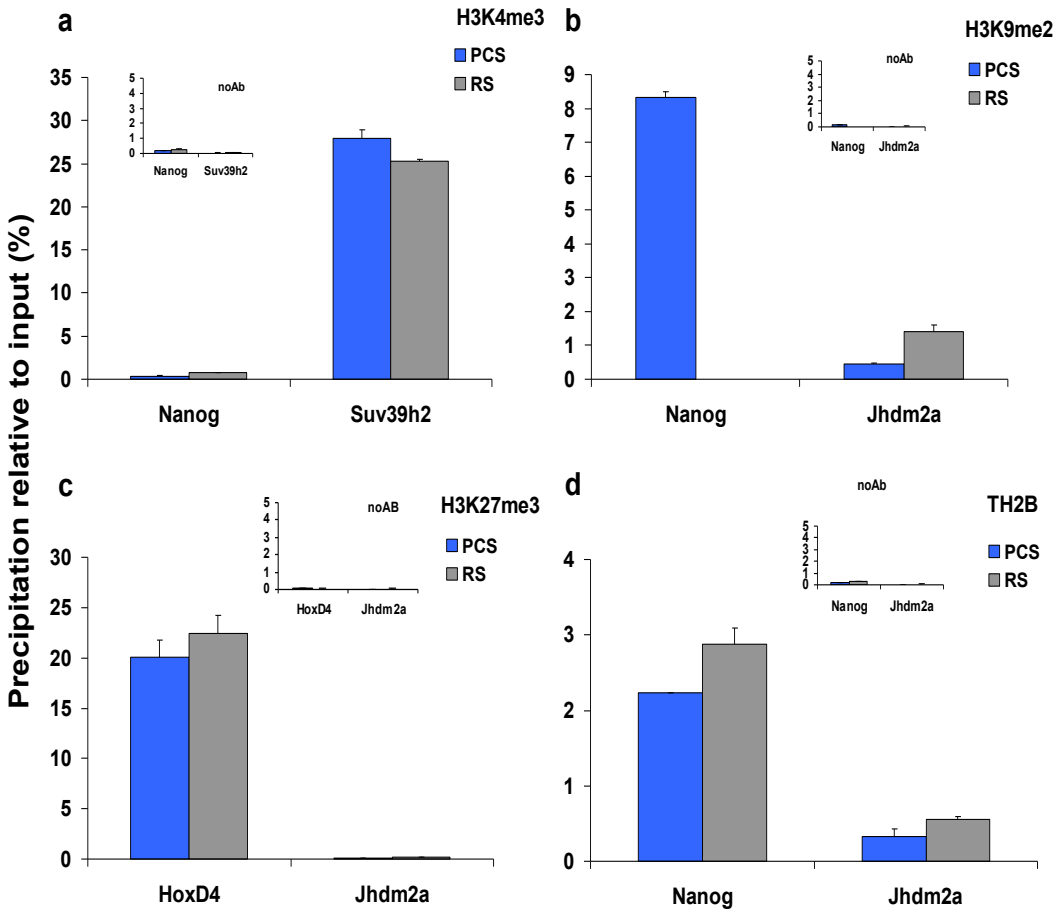

Figure 21: q-rtPCR on ChIP samples for ChIP-seq. ChIP was carried out with chromatin from PCS and RS. The precipitation efficiency of H3K4me3, H3K9me2, H3K27me3 and TH2B were assessed on genes known to have high and low enrichment for each histone modification or histone variant. The ChIP experiment was performed with two replicates for all samples, and data were analyzed by duplicate q-rtPCR for each replicate. Data are expressed as percent precipitation relative to input chromatin. Error bars indicate mean ± s.d. **a)** H3K4me3 enrichment on the Nanog and Suv39h2a promoter. **b)** H3K9me2 enrichment on the Nanog and *Jhdm2a* promoter. Due to a technical error, likely because template was not distributed to the relevant PCR plate wells, there was not obtained any results for H3K9me2 enrichment for round spermatids for the Nanog promoter **c)** H3K27me3 enrichment on the HoxD4 promoter and *Jhdm2a* promoter. **d)** TH2B enrichment on the Nanog and Suv39h2a promoter.

5.9 ChIP-sequencing

Immunoprecipitated DNA from PCS and RS was sent to BGI for HiSeq sequencing to obtain global maps of H3K4me3, H3K9me2, H3K27me3 and TH2B. The whole-genome ChIP sequencing was carried out with the Illumina/Solexa Genome Analyzer sequencing system.

The Illumina Hiseq sequencing gave on average 38,9 millions total reads for each sample, (Table 11, "total reads"), and 93 – 98% of the reads could be mapped to the genome (Table 11, "Mapped Rate").

Table 11: Results of reads alignment. Mapped reads: number of reads that can be aligned to reference genome. Unique mapped reads: number of reads which align to reference genome uniquely. Mapped rate: ratio of mapped reads to total reads. Unique mapped rate: ratio of unique mapped reads to total reads

Sample ID		Total Reads	Mapped Reads	Unique Mapped Reads	Mapped Rate	Unique Mapped Rate
1	TH2B PCS	38933003	37507869	30165593	96.34%	77.48%
2	TH2B PCS	38938756	37522214	30056500	96.36%	77.19%
3	H3K4me3 PCS	38887041	37007736	33594592	95.17%	86.39%
4	H3K4me3 PCS	38888524	36853628	33495940	94.77%	86.13%
5	H3K9me2 PCS	38911458	37483435	28597717	96.33%	73.49%
6	H3K9me2 PCS	38941864	37539154	28475033	96.40%	73.12%
7	H3K27me3 PCS	38933414	36471797	26061931	93.68%	66.94%
8	H3K27me3 PCS	38941130	36483472	25639733	93.69%	65.84%
9	Input PCS	38813548	37672837	30124447	97.06%	77.61%
10	TH2B RS	38949294	37473994	29579715	96.21%	75.94%
11	TH2B RS	38949961	37490387	29672908	96.25%	76.18%
12	H3K4me3 RS	38917299	37792522	32807465	97.11%	84.30%
13	H3K4me3 RS	38671616	37453261	32737724	96.85%	84.66%
14	H3K9me2 RS	38949745	37678440	29089361	96.74%	74.68%
15	H3K9me2 RS	38932573	37724822	29417768	96.90%	75.56%
16	H3K27me3 RS	38931263	36463143	25753499	93.66%	66.15%
17	H3K27me3 RS	38934909	36297213	24643293	93.23%	63.29%
18	Input RS	38919161	37699005	30043034	96.86%	77.19%

5.9.1 Genome-wide peak scanning

In genome-wide peak scanning (Table 12) mapped reads was used to identify regions significantly enriched for H3K4me3, H3K9me2, H3K27me3 and TH2B. The software was MACS version 1.4.0, used with default settings. A limited number of peaks were identified for TH2B and H3K9me2 for both PCS and RS. For H3K4me3, the average number of peaks found was higher for RS than PCS. In contrast there was identified more peaks in PCS than RS for the histone modification H3K27me3.

Table 12: Result of genome-wide peak scanning. Number of Peaks: the number of total peaks after peak calling. *Average (number of peaks)*: The average of total number of peaks for replicate sample. *Total Peaks Length (bp)*: the total length of all peaks. *Average (total peaks length (bp))*: The average of total peaks length for replicate sample.

Sample ID		Number of peaks	Average (number of peaks)	Total Peaks Length (bp)	Average (total peaks length (bp))
1	TH2B PCS	13	36	8541	24695
2	TH2B PCS	58		40849	
3	H3K4me3 PCS	38645	38779	98616381	97659067
4	H3K4me3 PCS	38912		96701752	
5	H3K9me2 PCS	81	137	58045	104304
6	H3K9me2 PCS	192		150563	
7	H3K27me3 PCS	16887	15499	41044813	39483078
8	H3K27me3 PCS	14111		37921343	
10	TH2B RS	53	80	38617	57497
11	TH2B RS	106		76377	
12	H3K4me3 RS	42564	43489	121881331	121536186
13	H3K4me3 RS	44413		121191041	
14	H3K9me2 RS	151	268	108621	196809
15	H3K9me2 RS	385		284997	
16	H3K27me3 RS	14301	13034	38673953	33888922
17	H3K27me3 RS	11766		29103890	

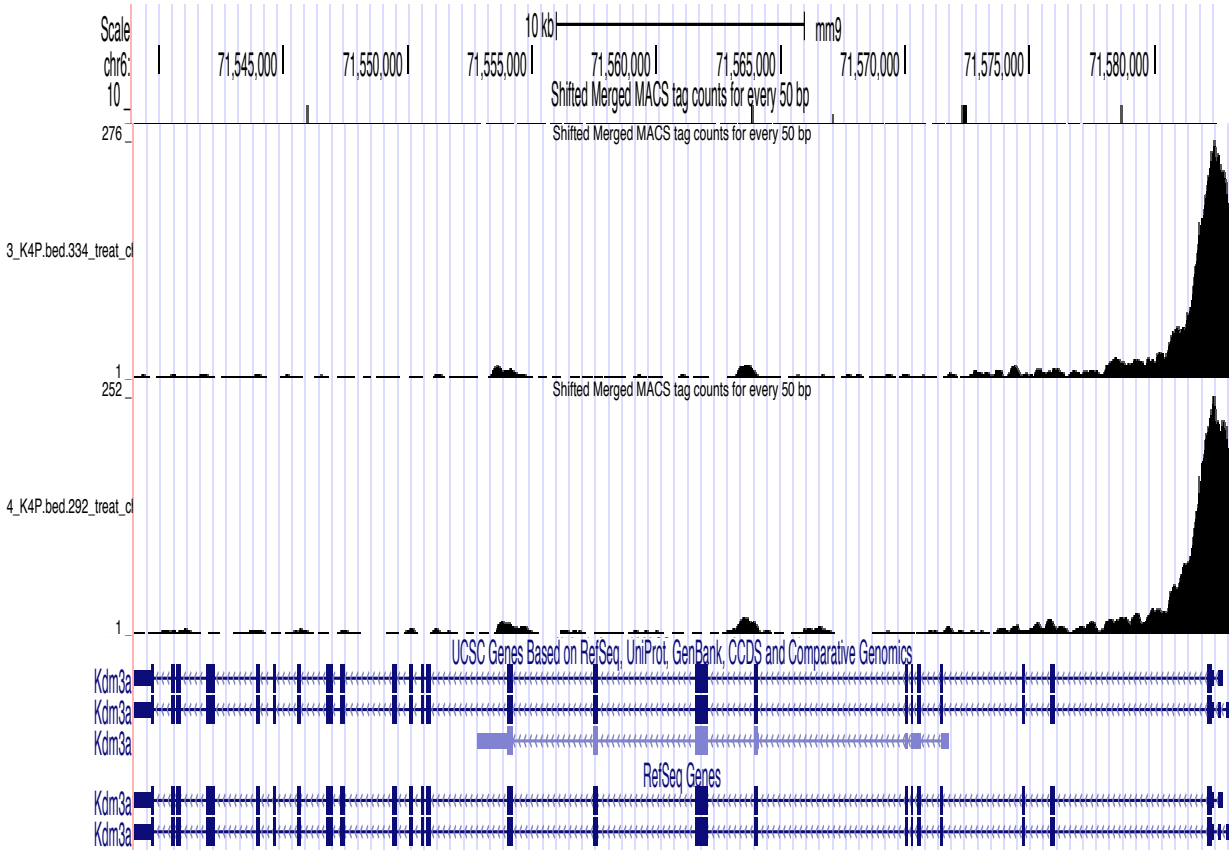

Figure 22: Visualization of uniquely mapped reads on the *Jhdm2a* (*Kdm3a*) gene for the histone modification H3K4me3 in PCS. As expected it is a peak in the transcription start sight of the *Jhdm2a* gene.

6 DISCUSSION

6.1 Initial optimization of ChIP assay

In this thesis, NCCIT cells were used for initial optimization of the ChIP-assay, as these cells can be easily obtained in large numbers, whereas PCS and RS are only available in limited amounts and require the sacrifice of mice and a cumbersome procedure for purification.

Sonication of chromatin is an important step in ChIP because the size of the chromatin fragments influences the resolution of the ChIP assay [85]. Chromatin fragments that are too long will decrease resolution and may cause noise, while too short fragments can be unsuitable for PCR, depending on amplicon length [66]. The sonication step is prone to variation between researchers as minor variation in the probe position in the 200 µl volume in the handheld 1,5 ml tube can result in significant differences in fragmentation efficiency. If the probe is positioned to high, close to the surface, it will result in foaming and dramatically reduced fragmentation of chromatin. Additionally, all the time the probe is touching the wall or bottom of the tube during sonication it will result in energy transfer to the plastic instead of efficient energy transfer to the chromatin solution. As shown with decreasing DNA size as a result of increasing sonication exposure in figure 10, substantial practice resulted in highly reliable chromatin fragmentation and therefore was an important achievement for the further work carried out in this thesis. The ideal fragment size for q-rtPCR is 200-1000 bp [85], and this was obtained with 10x30 sec sonication of NCCIT cells. Furthermore, it has previously been observed that when downscaling the starting cell number in ChIP the relative precipitation values increase, and this is reasoned to be due to an increased antibody-bead to chromatin ratio [66]. We confirmed this phenomenon when downscaling the cell number from 100 000 to 10 000 NCCIT cells (Fig. 11) in our ChIP experiments. Additionally, as expected due to increased stochastic variation in template amount, the standard deviation from the q-rtPCR increased when downscaling cell numbers. Further, it was previously observed that the NoAb background of unspecifically bound chromatin increases significantly when reducing the number of cells per ChIP. Here we overcame this problem through two steps providing increased stringency in the washing step of the chromatin-antibody-

bead complexes. i) Concentrations of SDS and NaCl in the RIPA buffer was raised from 0,1% and 140 mM to 0,24% and 490 mM, respectively. ii) Additionally, ChIP samples in PCR strips were vortexed thoroughly at full speed for 5 seconds each time after adding fresh washing solution and prior to the standard gentle head-over-tail rotation for 4 min. This combination of a physically and chemically more stringent washing procedure gave comparable background levels despite of a 10-fold reduction in cell numbers. Increased signal to noise ratio in the ChIP is an important achievement for laying the grounds for successful ChIP-seq.

6.2 Isolation and validation of PCS and RS

For the PCS, the size measured on the Countess® Automated Cell Counter was slightly lower than expected, however initial piloting experiments validated that the cell fraction obtained based on the reported size here mainly consisted of sex body containing PCS. The discrepancy between cell size measured on the Countess® Automated Cell Counter and that reported in the literature likely comes from the inaccuracy of the countess instrument. The purity of the PCS and RS was on average 83% and 82% respectively. Based on size and staining, the remaining fraction of the PCS is likely leptotene, zygotene and diplotene primary spermatocytes, and the remaining fraction of the round spermatids is most likely early round spermatids. Thus, although the fractions are not 100% pure PCS or Lectin PNA- containing RS, the remaining fraction consists of those cells that biologically are the most similar to the one we have aimed to isolate. Furthermore, our purities are comparable to the best reports in the literature.

6.3 Optimization of washing conditions for ChIP

In ChIP experiments it is desirable to achieve a high level of signal from the ChIP sample relative to the background signal (NoAb). A way to optimize the signal to noise ratio is to increase the stringency in the washing step.

The purpose of the washing steps is to remove non-specific binding of the chromatin so that only the specific interactions between antibody and its target protein remain. Stringency of the wash solution affects the amount of nonspecific binding that is washed away, and it is desirable that it is so stringent that as much as possible of the unspecific binding is removed, but at the same time it must not be so stringent that it interrupts the specific binding between antibody and antigen.

Various antibodies have different affinity for their target protein, so the stringency must be tested for each antibody used in a ChIP assay. In this thesis two washing solutions with differing degrees of stringency (RIPA-buffer with 140 mM NaCl and 0,1% SDS and RIPA-buffer with 490 mM NaCl and 0,24% SDS) were tested in ChIP with the antibodies H3K4me3, H3K9me2 and TH2B. As we received the H3K27me3 antibody used in this study after the other antibodies had already been through the 0.1% / regular stringency RIPA buffer experiments it was tested directly in ChIPs with high stringency RIPA buffer (RIPA buffer with 0,24% SDS). It performed very well under these conditions; hence, the results did not suggest a requirement for further testing. For H3K4me3 there was almost no difference in precipitation efficiency at increased stringency. On the contrary, for the H3K9me2 antibody, the stringency of the washing buffer had a major impact on the precipitation efficiency as increased stringency resulted in a 50% decrease in the precipitation efficiency. TH2B showed a slightly higher precipitation efficiency when washing with the 0,1% SDS buffer, but the signal to noise ratio between the sample and NoAb increased with about 50% when increasing the stringency. The stringency testing showed that increased stringency affected the various antibodies differently as reflected in the precipitation efficiency and the enrichment at the high target gene as compared to the low target.

6.4 Comparison of efficiency and specificity of ChIP antibodies

In ChIP analysis the antibody needs to be specific and efficient in the immunoprecipitation of a specific protein [85]. The affinity for epitopes differs between antibodies and thus affects the resulting signal levels. Also, antibodies may cross-react with similar eptiopes as the one they are intended to recognize. Papers that report the use of a specific antibody in ChIP may give a good indication of the suitability of an antibody, but it is important to notice that the quality of an antibody can differ between batches [86]. This is particularly important for polyclonal antibodies as different batches means that the antibodies have been raised in different animals and thus could perform very differently. Antibodies designated "ChIP-grade" or "ChIP qualified from the manufacturers also may not work successfully. Moreover, monoclonal and polyclonal antibodies are often available for the same epitope. A polyclonal antibody is derived from many different B cells, while a monoclonal antibody is derived from a single clone. Therefore, a polyclonal antibody population contains antibodies that recognize several different epitopes on the same protein or peptide, while a monoclonal antibody only recognize one epitope [85]. We wanted to identify the most promising commercially available antibodies for H3K4me3, H3K9me2, H3K27me3 and TH2B. The antibody used for H3K4me3 has previously been tested in our lab so there was no further testing required identifying this antibody. A monoclonal and a polyclonal H3K9me2 antibody from Diagenode were tested, and for the H3K27me3 modification three different antibodies were tested: a monoclonal and polyclonal antibody from Diagenode and a polyclonal antibody from Millipore. The polyclonal antibody gave the highest precipitation efficiency as compared to the monoclonal antibody for both H3K9me2 and H3K27me3, and this is consistent with the polyclonal antibody recognizing several epitopes on a protein, and that the combination of multiple recognition epitopes increases the likelihood of achieving high affinity interaction. The two polyclonal antibodies tested for H3K27me3, showed different precipitation efficiency in parallel ChIPs, indicating that there is a difference in the quality of the antibodies. The polyclonal antibody from Diagenode precipitated most chromatin, but this applied to loci with both high and low levels of H3K27me3. The antibody from Millipore performed better in distinguishing loci with high and low levels and thus gave the highest fold enrichment of high target relative to low target gene, so we chose to use this antibody for our

ChIP experiments. To our knowledge there exists only one commercial TH2B antibody validated for ChIP on the marked, so there was no further testing with this antibody.

As mentioned before, in ChIP, immunoprecipitation efficiency is antibody dependent and the level of precipitation cannot be directly compared between different antibodies. Therefore, although 40% precipitation is regarded as a high level of precipitation for some antibodies, a precipitation level of 4% can be a high level of precipitation for other antibodies and thus both rates of precipitation can reflect high chromatin levels.

6.5 Investigation of the role of TH2B, and the bivalent chromatin marks H3K27me3 and H3K4me3 in spermatogenesis

Previous experiments carried out in our lab showed that the *Hoxd4*, *Oct4* and *Nanog* genes are not expressed in PCS and RS. These aforementioned genes are all needed for early embryo development. We observe that there are lower levels of H3K4me3 on *Hoxd4* and *Oct4* in relation to the genes that are highly expressed in PCS and RS. Still the level is highly significantly above background. In the light of the study of Hammoud et al. [51], which reported that histone proteins are retained at developmentally important loci in sperm, it is appealing to speculate that the bivalent marks we observed on *Hoxd4* and *Oct4* reflects epigenetic preprogramming for early embryo development, as an analogue to the developmentally related preprogramming of embryonic and somatic stem cells [62]. Histone modifications at these loci may therefore be subject to transgenerational inheritance. However, one can not rule out the possibility that these marks are erased after fertilization and rewritten in the embryo. Another possibility is that the observed level at *Oct4* of H3K4me3 may reflect a previous state from when the gene was expressed in primordial germ cells [87]. In such a context it could be that H3K27me3 levels just have a role in repressing the genes throughout spermatogenesis. Moreover, in line with the lack of expression we also observed relatively high levels of the repressive H3K9me2 mark on the promoters of *Nanog, HoxD4 and Oct4*. A similar high occupancy was also observed for TH2B, which may indicate that TH2B has a repressive role. The chromatin

modifying enzymes encoding genes *Suv39h2*, *Meisetz*, *Jhdm2a* and *Hdac1* all have detectable levels of expression for both PCS and RS. As expected their promoters all harbor H3K4me3 and only background levels of the H3K27me3 mark. There are significant differences in the expression levels in this group of genes. This variation can not be explained through the levels of H3K27me3 and H3K4 methylation, however the expression levels seems to better follow the H3K9me2 levels, in particular for *Suv39h2a*, *Jhdm2a* and *Hdac1*. *Meisetz* is an exception to this trend. Furthermore, the TH2B levels are also relatively high for the lower expressed *Suv39h2* and *Meisetz* and lower for the more highly expressed *Jhdm2a* and *Hdac1*.

Taken together, the observed levels of TH2B and H3K9me2 at the promoters of the developmentally related genes and chromatin modifying enzymes are indicative of TH2B and H3K9me2 having a relationship with gene repression in PCS and RS.

Surprisingly, the relative highly expressed Prm1 gene harbored a low level of H3K4me3 and higher levels of TH2B, H3K9me2 and H3K27me3 than the other assessed genes which were expressed. One may speculate that the protamine gene is regulated differently from the other genes we analyzed and that this may be important for its unique biological role in the exchange of histones and chromatin packaging in spermatids.

Jhdm2a and *Hdac1* expression is comparable in PCS and RS. In accordance with this the levels of the various histone marks are also similar. Expression of *Suv39h2* and *Meisetz* increase almost 10 fold from the PCS to the RS stage. This however is not reflected in the histone modifications and variants assessed in this study and therefore the regulation of these genes are likely due to other regulatory factors, perhaps through DNA methylation or transcription factor binding or histone modifications not assessed here.

We observed that TH2B levels follow H3K9me2 levels seemingly well for all the genes we analyzed. Therefore correlation between these two histone marks was further investigated. For both PCS and RS although most strongly in RS we found good correlation between the repressive H3K9me2 and TH2B. This triggered a full analysis of the correlation between all the assessed epitopes. Also TH2B and H3K27me3 showed good correlations. Additionally we found negative correlation between TH2B and H3K4me3. Taken together, the aforementioned is supportive of that TH2B may have a role in testis specific gene repression.

6.6 Preparation of Chip DNA from spermatogenic cells for ChIP-Seq

6.6.1 Sonication

Although sonicating extensively a lower level of higher molecular DNA was still present in the chromatin samples used for ChiP-seq. However, this did not affect resolution of the ChIP-seq experiment as only a selected lower molecular weight fraction of the DNA was isolated after ChIP-seq library preparation. This selection was performed by electrophoresis where the size fraction of 200-500 bp was sliced out from the gel. Only this narrow range size of the samples was subjected to sequencing.

6.6.2 Technical aspects

Due to the substantial investment in time and money in ChIP-seq all ChIP samples and inputs were assessed for their quality by q-rtPCR prior to initiating HT-seq. To this end, a panel of genes shown to harbor high or low levels of the various histone modification or variants in our initial q-rtPCR investigation was analyzed. All ChIP samples showed the expected high or low enrichment of the antibody target, and they also showed low NoAb background levels, and therefore they were approved for library preparation and HT seq.

6.6.3 Bioinformatic analysis of ChIP-seq data

Illumina HiSeq successfully produced high numbers of reads that could be mapped to the genome. For all experiments 93-98% of the reads could be successfully mapped. Additionally, a high rate of sequencing reads where uniquely mapped to the genome, and these will be used for further analysis of localization of the histone modifications and the histone variant.

In the initial round of bioinformatics analysis only a limited number of peaks were identified for TH2B and H3K9me2 in the genome-wide peak scanning. The reason for this needs to be further investigated, but it is likely that the default settings used for peak calling is unsuitable for analysis of TH2B and H3K9me2. We expect that

tailored analysis settings adjusted to peak width, peak height and peak distribution for each of TH2B and H3K9me2 will allow for more sensitive detection of genomic loci with high levels of these modifications. Through discussions with researchers experienced in ChIP-seq analysis it is become clear to us that the analysis of many modifications requires adjustment of default settings.

In contrast to a previous report from *Godmann et al. 2007* [46] showing low global H3K4me3 levels observed by immunocytochemistry in pachytene spermatocytes, we only observed a slightly lower level as compared to RS. We observed a 25% lower genomic occupancy of H3K4me3 in PCS as compared to RS, measured by the number of base pairs in the genome represented in region identified as H3K4me3 peaks (data not shown). The lower level was due to a combination of slightly reduced peak width and a lower number of peaks. A possible explanation of the discrepancy between our data and those of *Godmann et al.* [46] could be the difference in H3K4me3 antibodies used in each study.

Additionally immunocytochemistry generally has a lower sensitivity than ChIP. One may also imagine that the global levels observed by *Godman et al*., could be due to chromatin binding proteins blocking the many of H3K4me3 epitopes thus making them unavailable to antibody binding in immunocytochemistry assays. After stringent lysis and then sonication procedure of ChIP chromatin, these chromatin binding proteins can potentially be removed and therefore the epitope become available for immunoprecipitation. This is an appealing explanation as H3K4me3 sites located outside promoters and other regulatory genomic elements have been identified as hotspots for double strand break related to meiotic recombination [88].

Due to the limited time available for the work carried out for this thesis, additionally analysis of ChIP-Seq data will be carried out after the completion of this thesis. However, a preliminary glimpse into the data as shown in figure 22, which visualize uniquely mapped reads of DNA pulled down in two ChIP experiments, indicate successful ChIP and library preparation for high throughput sequencing.

6.7 Conclusion and outlook

During the progression of spermatogenesis canonical histones are replaced by histone variants, and at the end of spermatogenesis, most histones are replaced by protamines. However, it has been shown that a small fraction of histones are retained in sperm chromatin. Interestingly, the testis-specific histone variant TH2B has been detected at retained nucleosomes [51]. To date the function of TH2B is not known, but TH2B has been proposed to have function in chromatin organization. Our data indicate that TH2B may play a role as a testis specific repressive histone variant, as we observe good correlation with the two repressive histone modifications H3K9me2 and H3K27me3, and negative correlation with the activating mark H3K4me3.

We also observed significant levels of the bivalent marks H3K4me3 and H3K27me3 on the *Hoxd4* and *Oct4* promoter in PCS and RS. On a speculative note, this could perhaps be suggestive of preprogramming for expression in early embryo development.

This work has laid the grown for extensive analysis of three histone modifications H3K4me3, H3K9me2, H3K27me3 and the histone variant TH2B in PCS and RS. The massive amount of obtained data from whole genome sequencing will likely allow for increased understanding of the role of the investigated histone modifications and variants in spermatogenesis.

REFERENCE LIST

1. Goldberg, A.D., C.D. Allis, and E. Bernstein, *Epigenetics: a landscape takes shape.* Cell, 2007. **128**(4): p. 635-8.
2. Luger, K., et al., *Crystal structure of the nucleosome core particle at 2.8 A resolution.* Nature, 1997. **389**(6648): p. 251-60.
3. Bottomley, M.J., *Structures of protein domains that create or recognize histone modifications.* EMBO Rep, 2004. **5**(5): p. 464-9.
4. Allis, C.D., Jenuwein, T and Reinberg, D, *Epigenetics*2007: New York: Cold Spring Harbour Labaratory Press.
5. Kosak ST , G.M. *Form follows function: the genomic organization of cellular differentiation*. , 2004. **18**, 1371-1384 DOI: 10.1101/gad.1209304.
6. Stamm, S., et al., *Function of alternative splicing.* Gene, 2005. **344**: p. 1-20.
7. Kadonaga, J.T., *Regulation of RNA polymerase II transcription by sequence-specific DNA binding factors.* Cell, 2004. **116**(2): p. 247-57.
8. Lusser, A. and J.T. Kadonaga, *Chromatin remodeling by ATP-dependent molecular machines.* Bioessays, 2003. **25**(12): p. 1192-200.
9. Kim, S.H., et al., *Spatial genome organization during T-cell differentiation.* Cytogenet Genome Res, 2004. **105**(2-4): p. 292-301.
10. He, L. and G.J. Hannon, *MicroRNAs: small RNAs with a big role in gene regulation.* Nat Rev Genet, 2004. **5**(7): p. 522-31.
11. Okamura, K. and E.C. Lai, *Endogenous small interfering RNAs in animals.* Nat Rev Mol Cell Biol, 2008. **9**(9): p. 673-8.
12. Zamore, P.D. and B. Haley, *Ribo-gnome: the big world of small RNAs.* Science, 2005. **309**(5740): p. 1519-24.
13. Gan, Q., et al., *Concise review: epigenetic mechanisms contribute to pluripotency and cell lineage determination of embryonic stem cells.* Stem Cells, 2007. **25**(1): p. 2-9.
14. Zamudio, N.M., S. Chong, and M.K. O'Bryan, *Epigenetic regulation in male germ cells.* Reproduction, 2008. **136**(2): p. 131-46.
15. Kouzarides, T., *Chromatin modifications and their function.* Cell, 2007. **128**(4): p. 693-705.
16. Strahl, B.D. and C.D. Allis, *The language of covalent histone modifications.* Nature, 2000. **403**(6765): p. 41-5.
17. Bannister, A.J. and T. Kouzarides, *Regulation of chromatin by histone modifications.* Cell Res, 2011. **21**(3): p. 381-95.
18. Fernandez-Capetillo, O., et al., *H2AX is required for chromatin remodeling and inactivation of sex chromosomes in male mouse meiosis.* Dev Cell, 2003. **4**(4): p. 497-508.
19. Ng, S.S., et al., *Dynamic protein methylation in chromatin biology.* Cell Mol Life Sci, 2009. **66**(3): p. 407-22.
20. Bernstein, B.E., A. Meissner, and E.S. Lander, *The mammalian epigenome.* Cell, 2007. **128**(4): p. 669-81.
21. Margueron, R., P. Trojer, and D. Reinberg, *The key to development: interpreting the histone code?* Curr Opin Genet Dev, 2005. **15**(2): p. 163-76.

22. Nakao, M., *Epigenetics: interaction of DNA methylation and chromatin.* Gene, 2001. **278**(1-2): p. 25-31.
23. Eden, S. and H. Cedar, *Role of DNA methylation in the regulation of transcription.* Curr Opin Genet Dev, 1994. **4**(2): p. 255-9.
24. Okano, M., et al., *DNA methyltransferases Dnmt3a and Dnmt3b are essential for de novo methylation and mammalian development.* Cell, 1999. **99**(3): p. 247-57.
25. Jenkins, T.G. and D.T. Carrell, *The paternal epigenome and embryogenesis: poising mechanisms for development.* Asian J Androl, 2011. **13**(1): p. 76-80.
26. Bird, A., *DNA methylation patterns and epigenetic memory.* Genes Dev, 2002. **16**(1): p. 6-21.
27. Hendrich, B. and S. Tweedie, *The methyl-CpG binding domain and the evolving role of DNA methylation in animals.* Trends Genet, 2003. **19**(5): p. 269-77.
28. Zhao, W., et al., *The essential role of histone H3 Lys9 di-methylation and MeCP2 binding in MGMT silencing with poor DNA methylation of the promoter CpG island.* J Biochem, 2005. **137**(3): p. 431-40.
29. Montellier, E., et al., *Histone crotonylation specifically marks the haploid male germ cell gene expression program: post-meiotic male-specific gene expression.* Bioessays, 2012. **34**(3): p. 187-93.
30. de Kretser, D.M., Loveland, K.L., Meinhardt A., Simorangkir D. and Wreford, N., *Spermatogenesis.* Human Reproduction, 1998. **13**: p. Supplement 1.
31. Clermont, Y., *Kinetics of spermatogenesis in mammals: seminiferous epithelium cycle and spermatogonial renewal.* Physiol Rev, 1972. **52**(1): p. 198-236.
32. de Kretser, D.K.J., *Cytology of the testis.* The Physiology of Reproduction, 1994.
33. Cobb, J. and M.A. Handel, *Dynamics of meiotic prophase I during spermatogenesis: from pairing to division.* Semin Cell Dev Biol, 1998. **9**(4): p. 445-50.
34. Roeder, G.S., *Meiotic chromosomes: it takes two to tango.* Genes Dev, 1997. **11**(20): p. 2600-21.
35. Morelli, M.A. and P.E. Cohen, *Not all germ cells are created equal: aspects of sexual dimorphism in mammalian meiosis.* Reproduction, 2005. **130**(6): p. 761-81.
36. Baarends, W.M. and J.A. Grootegoed, *Chromatin dynamics in the male meiotic prophase.* Cytogenet Genome Res, 2003. **103**(3-4): p. 225-34.
37. Sasaki, H. and Y. Matsui, *Epigenetic events in mammalian germ-cell development: reprogramming and beyond.* Nat Rev Genet, 2008. **9**(2): p. 129-40.
38. Seki, Y., et al., *Extensive and orderly reprogramming of genome-wide chromatin modifications associated with specification and early development of germ cells in mice.* Dev Biol, 2005. **278**(2): p. 440-58.
39. Carrell, D.T. and S.S. Hammoud, *The human sperm epigenome and its potential role in embryonic development.* Mol Hum Reprod, 2010. **16**(1): p. 37-47.

40. Peters, A.H., et al., *Loss of the Suv39h histone methyltransferases impairs mammalian heterochromatin and genome stability.* Cell, 2001. **107**(3): p. 323-37.
41. Lachner, M. and T. Jenuwein, *The many faces of histone lysine methylation.* Curr Opin Cell Biol, 2002. **14**(3): p. 286-98.
42. O'Carroll, D., et al., *Isolation and characterization of Suv39h2, a second histone H3 methyltransferase gene that displays testis-specific expression.* Mol Cell Biol, 2000. **20**(24): p. 9423-33.
43. Tachibana, M., et al., *Set domain-containing protein, G9a, is a novel lysine-preferring mammalian histone methyltransferase with hyperactivity and specific selectivity to lysines 9 and 27 of histone H3.* J Biol Chem, 2001. **276**(27): p. 25309-17.
44. Tachibana, M., et al., *Functional dynamics of H3K9 methylation during meiotic prophase progression.* EMBO J, 2007. **26**(14): p. 3346-59.
45. Hayashi, K., K. Yoshida, and Y. Matsui, *A histone H3 methyltransferase controls epigenetic events required for meiotic prophase.* Nature, 2005. **438**(7066): p. 374-8.
46. Godmann, M., et al., *Dynamic regulation of histone H3 methylation at lysine 4 in mammalian spermatogenesis.* Biol Reprod, 2007. **77**(5): p. 754-64.
47. Ciccone, D.N., et al., *KDM1B is a histone H3K4 demethylase required to establish maternal genomic imprints.* Nature, 2009. **461**(7262): p. 415-8.
48. Okada, Y., et al., *Histone demethylase JHDM2A is critical for Tnp1 and Prm1 transcription and spermatogenesis.* Nature, 2007. **450**(7166): p. 119-23.
49. Kimmins, S. and P. Sassone-Corsi, *Chromatin remodelling and epigenetic features of germ cells.* Nature, 2005. **434**(7033): p. 583-9.
50. Wouters-Tyrou, D., et al., *Nuclear basic proteins in spermiogenesis.* Biochimie, 1998. **80**(2): p. 117-28.
51. Hammoud, S.S., et al., *Distinctive chromatin in human sperm packages genes for embryo development.* Nature, 2009. **460**(7254): p. 473-8.
52. Brykczynska, U., et al., *Repressive and active histone methylation mark distinct promoters in human and mouse spermatozoa.* Nat Struct Mol Biol, 2010. **17**(6): p. 679-87.
53. Doenecke, D., et al., *Histone gene expression and chromatin structure during spermatogenesis.* Adv Exp Med Biol, 1997. **424**: p. 37-48.
54. Martianov, I., et al., *Polar nuclear localization of H1T2, a histone H1 variant, required for spermatid elongation and DNA condensation during spermiogenesis.* Proc Natl Acad Sci U S A, 2005. **102**(8): p. 2808-13.
55. Yan, W., et al., *HILS1 is a spermatid-specific linker histone H1-like protein implicated in chromatin remodeling during mammalian spermiogenesis.* Proc Natl Acad Sci U S A, 2003. **100**(18): p. 10546-51.
56. Celeste, A., et al., *Genomic instability in mice lacking histone H2AX.* Science, 2002. **296**(5569): p. 922-7.
57. Handel, M.A., *The XY body: a specialized meiotic chromatin domain.* Exp Cell Res, 2004. **296**(1): p. 57-63.
58. Turner, J.M., et al., *BRCA1, histone H2AX phosphorylation, and male meiotic sex chromosome inactivation.* Curr Biol, 2004. **14**(23): p. 2135-42.
59. Lu, S., et al., *Mass spectrometry analysis of dynamic post-translational modifications of TH2B during spermatogenesis.* Mol Hum Reprod, 2009. **15**(6): p. 373-8.

60. Zalensky, A.O., et al., *Human testis/sperm-specific histone H2B (hTSH2B). Molecular cloning and characterization.* J Biol Chem, 2002. **277**(45): p. 43474-80.
61. Azuara, V., et al., *Chromatin signatures of pluripotent cell lines.* Nat Cell Biol, 2006. **8**(5): p. 532-8.
62. Bernstein, B.E., et al., *A bivalent chromatin structure marks key developmental genes in embryonic stem cells.* Cell, 2006. **125**(2): p. 315-26.
63. Mikkelsen, T.S., et al., *Genome-wide maps of chromatin state in pluripotent and lineage-committed cells.* Nature, 2007. **448**(7153): p. 553-60.
64. Pan, G., et al., *Whole-genome analysis of histone H3 lysine 4 and lysine 27 methylation in human embryonic stem cells.* Cell Stem Cell, 2007. **1**(3): p. 299-312.
65. Zhao, X.D., et al., *Whole-genome mapping of histone H3 Lys4 and 27 trimethylations reveals distinct genomic compartments in human embryonic stem cells.* Cell Stem Cell, 2007. **1**(3): p. 286-98.
66. Dahl, J.A. and P. Collas, *A rapid micro chromatin immunoprecipitation assay (microChIP).* Nat Protoc, 2008. **3**(6): p. 1032-45.
67. Collas, P., *The current state of chromatin immunoprecipitation.* Mol Biotechnol, 2010. **45**(1): p. 87-100.
68. Orlando, V., *Mapping chromosomal proteins in vivo by formaldehyde-crosslinked-chromatin immunoprecipitation.* Trends Biochem Sci, 2000. **25**(3): p. 99-104.
69. Collas, P. and J.A. Dahl, *Chop it, ChIP it, check it: the current status of chromatin immunoprecipitation.* Front Biosci, 2008. **13**: p. 929-43.
70. Ravindranath, N. and M. Dym, *Isolation of rat ventral prostate basal and luminal epithelial cells by the STAPUT technique.* Prostate, 1999. **41**(3): p. 173-80.
71. Bellve, A.R., et al., *Spermatogenic cells of the prepuberal mouse. Isolation and morphological characterization.* J Cell Biol, 1977. **74**(1): p. 68-85.
72. Inc., P. *STA-PUT, Velocity Sedimentation Cell Separator for Rapid, Easy Cell Separation*. [Internet communication]; Available from: http://tecniglas.com/images/STA-PUT.2008.Cdn.Information.pdf.
73. Miller, R.G. and R.A. Phillips, *Separation of cells by velocity sedimentation.* Journal of Cellular Physiology, 1969. **73**: p. 191-202.
74. biosystems, a. *Power SYBR® Green PCR Master Mix and Power SYBR® Green RT-PCR Reagents Kit, Users Guide*. [Internet communication]; Available from: https://tools.invitrogen.com/content/sfs/manuals/cms_042179.pdf.
75. Qiagen. *Real-time RT-PCR using SYBR Green based detection*. [Internet communication]; Available from: http://www.qiagen.com/literature/qiagennews/weeklyarticle/06_09/e14/popup.aspx.
76. Invitrogen. *qPCR vs. Digital PCR vs. Traditional PCR*. Available from: http://www.invitrogen.com/site/us/en/home/Products-and-Services/Applications/PCR/real-time-pcr/qpcr-education/qpcr-vs-digital-pcr-vs-traditional-pcr.html.
77. MRC, M.R.C., Inc. *RNAzol® RT* [Internet Communication]; Available from: http://www.mrcgene.com/rnazol.htm.

78. Invitrogen. *TURBO DNA-freeTM Kit* [Internet Communication]; Available from: http://tools.invitrogen.com/content/sfs/manuals/cms_055740.pdf.
79. Thermo-Scientific. *NanoDrop 1000 Spectrophotometer V.3.7 Users`manual*. [Internet communication]; Available from: http://www.nanodrop.com/library/nd-1000-v3.7-users-manual-8.5x11.pdf.
80. AppliedBiosystems. *High Capacity cDNA Reverse Transcription Kits For 200 and 1000 Reactions Protocol*. [Internet communication]; Available from: http://www3.appliedbiosystems.com/cms/groups/mcb_support/documents/generaldocuments/cms_042557.pdf.
81. Invitrogen. *Qubit® 2.0 Fluorometer, User Manual*. [Internet communication]; Available from: http://www.invitrogen.com/etc/medialib/en/filelibrary/cell_tissue_analysis/Qubit-all-file-types.Par.0519.File.dat/Qubit-2-Fluorometer-User-Manual.pdf.
82. illumina. *TruSeqTM RNA and DNA Sample Preparation Kits v2*. [Internet Communication]; Available from: http://www.illumina.com/documents/%5Cproducts%5Cdatasheets%5Cdatasheet_truseq_sample_prep_kits.pdf.
83. Illumina. *Preparing Samples for ChIP Sequencing of DNA*. [Internet communication]; Available from: http://grcf.jhmi.edu/hts/protocols/11257047_ChIP_Sample_Prep.pdf.
84. Cullum, R., O. Alder, and P.A. Hoodless, *The next generation: using new sequencing technologies to analyse gene regulation.* Respirology, 2011. **16**(2): p. 210-22.
85. abcam. *A beginners guide to ChIP*. [Internet Communication]; Available from: http://docs.abcam.com/pdf/chromatin/A-beginners-guide-to-ChIP.pdf.
86. Haring, M., et al., *Chromatin immunoprecipitation: optimization, quantitative analysis and data normalization.* Plant Methods, 2007. **3**: p. 11.
87. Hajkova, P., et al., *Chromatin dynamics during epigenetic reprogramming in the mouse germ line.* Nature, 2008. **452**(7189): p. 877-81.
88. Brick, K., et al., *Genetic recombination is directed away from functional genomic elements in mice.* Nature, 2012. **485**(7400): p. 642-5.